Morten Skogvold

Supervisory-switched Control for Dynamic Positioning Systems in Arctic Areas

Trondheim June 2010

Master´s Thesis

NTNU
Norwegian University of Science and Technology
Faculty of Engineering Science and Technology
Department of Marine Technology

NTNU
Norwegian University of Science and Technology

MASTER THESIS IN MARINE CYBERNETICS

SPRING 2010

FOR

MORTEN SKOGVOLD

Supervisory-switched control for dynamic positioning systems in arctic areas

Work description

The environmental forces ships operating in arctic areas experiences vary from normal open water conditions to various types of ice forces. For a dynamic positioning (DP) system to work optimally in these very different conditions, it may not be sufficient to use classic control strategies developed mainly for open water. Hybrid control has shown promising results for the transition between ice regimes and should be further investigated. For control of the ship inside an ice regime, there is a need for better control algorithms based on the nature of the ice forces.

For simulation of the system, the MCSim simulator in Matlab/Simulink will be used. MCSim should be extended to include ice ridge loads in addition to broken and level ice and combinations of different ice regimes. This would make it possible to simulate the ice conditions more realistically as the ice condition usually is a combination of different ice regimes.

Scope of work

1. Investigate control strategies and develop controllers and estimators for control of ships in broken ice, level ice and ice ridges.
2. Develop a supervisory control system for accurate switching between ice controllers and observers including bumpless transfer of control signal.
3. Simulate the complete system in a realistic arctic environment using MCSim.
4. Perform a parameter sensitivity analysis of the hybrid control system.

The report shall be written in English and edited as a research report including literature survey, description of mathematical models, description of control algorithms, simulation results, model test results, discussion and a conclusion including a proposal for further work. Source code should be provided on a CD with code listing enclosed in appendix. It is supposed that Department of Marine Technology, NTNU, can use the results freely in its research work, unless otherwise agreed upon, by referring to the student's work.

The thesis should be submitted in two copies within June 21st.

Advisor: Dr. Trong Dong Nguyen, Marine Cybernetics

Supervisor: Professor Asgeir J. Sørensen

Abstract

Dynamically positioned vessels may experience rapidly changing environmental loads if the vessels are operating in ice-covered waters. The transition between open water to level ice is an abrupt change from no ice loads to forces up to several hundred kN in only a few seconds. If vessels are to operate in such conditions, there is a need to develop new technologies for dynamic positioning (DP) control systems which takes these varying loads into consideration. The work presented in this master's thesis is aimed towards the subject of supervisory control applied to dynamic positioning systems for arctic areas.

A supervisory-switched DP control system, including combined bumpless transfer and anti-windup control scheme adapted for use in a DP control, is developed. A method for estimation of operating regime based on spectral analysis of vessel pitch motion measurements is developed through a simulation study of the vessel motion in level ice. The supervisory control system is tested and compared with an open water DP system in a simulation study where the vessel behavior is simulated in the transition from open water to level ice and vice versa. The simulation study shows that the supervisory-switched control system reduces the deviation from the reference position from 4 meters to 1.5 meters in surge direction when the ice hits the vessel head on.

A variation of parameters in the supervisor shows that the ice detection time is dependent on the length of the buffered pitch measurement signal. Shorter buffer length gives rapid adaptation, but the ability to separate different operating regimes is sensitive to the resolution of the spectral analysis, and thus the buffer length should not be too short.

A simulation of ice drifting towards the vessel with a relative angle to the vessel shows that the vessel is not capable of keeping the heading when the ice hits the vessel sides and experiences a loss of position. Simulation of a supervisory-switched controller which switches to a weather-optimal positioning control scheme (WOPC) when the ice hits from an angle shows that the vessel is able to solve the problem of ice drifting from an angle by rotating the bow towards the resulting ice loads when the ice sheet hits and thus is able to keep the position.

Acknowledgements

This thesis is written during the spring of 2010 as a final part of my master's studies in marine technology at the Norwegian University of Science and Technology in Trondheim.

I would like to thank Petter Stuberg and dr. Dong Trong Nguyen at Marine Cybernetics for many inspiring and helpful discussions on the subject of ice modeling, supervisory control and DP systems in general. Their suggestions and input on the implementation of the control system in MATLAB/Simulink is also acknowledged.

Sverre Wendt Slettebø and Sindre Ueland have also been working on a thesis regarding ice modeling and DP control in the spring of 2010. We have had many illuminating discussions on the subjects of DP control systems.

Finally, I would like to thank my supervisor, professor Asgeir J. Sørensen for valuable motivation and suggestions in writing this thesis. His many advices on research and life in general are much appreciated, as are also his inputs on proper report writing.

Morten Skogvold
Trondheim, June 18, 2010

Contents

Abstract III
Acknowledgements V
List of figures X
List of tables XII
1 Introduction 1
1.1 Background and motivation 1
1.2 Previous work and published literature 3
1.3 Contributions 3
1.4 Outline of thesis 3
2 Supervisory control 5
2.1 Formal definition 6
2.2 The switched system 6
2.2.1 Matching property 6
2.2.2 Detectability property 6
2.3 The supervisor 7
2.3.1 Multi-estimator 7
2.3.2 Monitoring signal 7
2.3.3 Switching 8
2.3.4 Small error property 9
2.3.5 Non-destabilization property 9
2.4 Bumpless transfer 10
2.4.1 Concept 10
2.4.2 Implementation issues 12
2.4.3 Gain calculation by LMIs 13
3 Ice 15
3.1 Ice detection 15
3.1.1 Sensors 15
3.1.2 Dynamic models 17
3.1.3 Spectral analysis 18

3.2 Level ice 18
3.2.1 Level ice load frequencies 18
3.2.2 Proposed level ice frequency model 25
3.3 Broken Ice 26
3.4 Open water 26
3.4.1 Pitch frequency response in waves 26
4 Supervisory-switched DP control system design 31
4.1 Observer design 31
4.1.1 Open water observer 31
4.1.2 Ice observers 32
4.2 Control law design 33
4.2.1 PID controller 33
4.2.2 Weather-optimal positioning control 33
4.3 Supervisor 35
4.3.1 FFT and buffer 35
4.3.2 Switching logic 36
5 Simulation study 37
5.1 Input data 37
5.1.1 Vessel model 37
5.1.2 Simulation setup 37
5.2 Results 40
5.2.1 Case 1: Traditional control comparison 40
5.2.2 Case 2: Supervisory switching 42
5.3 Variation of parameters 45
5.3.1 Buffer time 45
5.3.2 Forgetting factors 47
5.3.3 Hysteresis constant 48
5.4 Ice drift angle 48
5.4.1 Case 3: Supervisory control using PID controllers 49
5.4.2 Case 4: Supervisory control with WOPC 50
5.5 Discussion 52
6 Conclusion and further work 55

6.1 Conclusion 55
6.2 Recommendations for further work 55
7 References 57
Appendix A Weather optimal positioning control 59
Appendix B Control system parameters 62
Appendix C Contents of the attached CD 65

List of figures

Figure 1 Station keeping in the central polar pack, 2004 (Keinonen, 2008) 2
Figure 2 Supervisory control 5
Figure 3 Supervisor components with dynamical systems 7
Figure 4 dwell-time switching logic (Hespanha, 2002) 8
Figure 5 Scale-independent hysteresis switching logic (Hespanha, 2002) 9
Figure 6 Bumpless transfer scheme (based on Zaccarian & Teel (2002)) 11
Figure 7 Visual observation of ice conditions 17
Figure 8 Pitch level ice loads and vessel response 20
Figure 9 Pitch ice loads and vessel response frequency spectra 20
Figure 10 Pitch level ice loads and vessel response zoom-in 21
Figure 11 Pitch level ice loads (top) and vessel response (bottom) for 0.3 m/s drift velocity 22
Figure 12 Pitch ice loads spectrum (top) and vessel response frequency spectrum (bottom) for 0.3 m/s drift velocity 22
Figure 13 Pitch ice loads spectrum (top) and vessel response frequency spectrum (bottom) for 0.5 m/s drift velocity 23
Figure 14 Ice pitch ice loads spectrum (top) and vessel response frequency spectrum (bottom) for 0.7 m/s drift velocity 24
Figure 15 Pitch response frequency spectrum for fast ice drift 24
Figure 16 Proposed level ice pitch frequency model 26
Figure 17 Open water pitch response 27
Figure 18 Pitch motion time series (top) and FFT (bottom) for open water simulation without waves 28
Figure 19 Proposed open water pitch frequency model 29
Figure 20 Weather optimal positioning motivated by a pendulum (Fossen & Strand, 2000) 34
Figure 21 Supervisor components with FFT 35
Figure 22 Ice drifting events 39
Figure 23 Ice drift angle sketch 40
Figure 24 Level ice test surge ice loads 40
Figure 25 Open water - level ice using traditional control 41
Figure 26 Open water controller commanded force 41
Figure 27 Open water controller PID terms 42
Figure 28 OW-LI-OW Monitoring signals and switching signal 42
Figure 29 OW-LI-OW Position time series 43
Figure 30 Surge velocity estimate comparison 44
Figure 31 Control commands 44
Figure 32 Detection time vs. buffer time 46
Figure 33 Results from λ_{LI}=0.15 47
Figure 34 Results from λ_{LI}=0.20 48
Figure 35 Monitoring signal and switching signal 49
Figure 36 Position time series 50
Figure 37 Monitoring signal and switching signal 50

Figure 38 Missing ice breaking loads 51
Figure 39 Position and reference 51
Figure 40 Control forces 52

List of tables

Table 1 MC Supply dimensions 19
Table 2 Level ice conditions 19
Table 3 Environmental conditions for open water with waves 26
Table 4 Current simulation environmental conditions 27
Table 5 MC Supply dimensions 37
Table 6 Open water test environmental forces 38
Table 7 Level ice condition 38
Table 8 Description of simulation cases 38

1 Introduction

This chapter presents the background and motivation for studying dynamical positioning (DP) systems and why supervisory-switched control is of interest in continuity of this. Next, a review of the available literature relevant for this master thesis is given. The chapter ends with a presentation of the contribution of the present work and an outline of this thesis.

1.1 Background and motivation

As the level of known oil reserves in the world are decreasing and the demand for oil is still high, the oil companies are searching for oil in more demanding areas. The trend in the oil industry is to go deeper and into harsher climates. Promising areas in terms of finding new oil and gas fields include the arctic areas. The U.S. Geological Survey (USGS Release, 2008) estimates that the area north of the arctic circle holds about 22 percent of the worlds undiscovered, technically recoverable oil and gas resources. Out of these resources, 84 percent are expected to occur offshore. This trend calls for more advanced technologies combining experiences from offshore and arctic operations to be developed.

The Arctic is a sea surrounded by continents. It has some of the world's most demanding environmental conditions characterized by long, cold winters and short summers. Some parts of the Arctic is covered by ice year-round, and most of the Arctic experience long periods of some form of ice cover on the sea surface. There are several definitions on where the arctic area border is. Some say that it is where there exists sea ice cover, others that it is at 60 degrees north or at the 10 degree Celsius isotherm in July.

To be able to perform oil exploration and production in the arctic areas, there is a need for vessels capable of holding their position even in the presence of ice. This is needed to perform drilling operations and loading and offloading between vessels. The vessels need to be able to keep position either with the help of ice breakers or, ideally, on their own. When vessels perform station keeping, a (DP) system is used to automatically calculate the necessary thruster action to keep the position. If the vessel operates without assistance from ice breakers, a conventional DP system may not perform satisfactory due to large load variations.

Some experiences from full-scale trials of DP ice operations with and without ice breaker assistance is given by Keinonen (2008) where the main focus is on development of a functional ice management program. An ice breaker using an open water DP system was proved not workable in severe ice conditions. For a vessel to operate independent of ice breaker assistance, there is a need for development of DP systems tailored for operation in ice-covered waters.

Figure 1 Station keeping in the central polar pack, 2004 (Keinonen, 2008)

The sea ice can be divided into several different regimes, and is normally classified as broken ice, level ice, ice ridges or ice bergs. The ice conditions experienced in the arctic areas are normally combinations of some of these ice types. A vessel operating near the ice edge can therefore experience large variations in load characteristics. If the vessel passes from open water into the ice, the forces will change drastically. Also passing through different types of ice, will give different load characteristics. The DP control algorithm should be able to react to the varying loads, and adapt the controller action to the changes.

The concept of adaptive control has been studied since the early 1950s and adaptive control techniques have been used commercially from around 1980 (Åstrøm & Wittenmark, 1995). An example of successful use of adaptive control techniques is the gain scheduling procedure used in autopilots for aircrafts where different operating conditions need different controller gains.

However, the traditional adaptive control theory has a number of limitations. The controllers used need to be a continuously parameterized family of controllers that in some way reflects the changing operating conditions of the process (Hespanha et al., 2003). This can be difficult to obtain in complex systems without clearly defined parameters representative for the changing operating conditions.

An alternative to the continuous adaptation is to perform a discrete switching between a number of controllers. This leads to the logic-based switching and supervisory control used for switching between open water and ice controllers in this thesis. Supervisory control makes the system capable of more rapid adaptation and separates the supervision problem from the control problem. The natural modularity of the systems also makes it possible to use well tested "off-the-shelf" control laws for the different operating conditions. The control system can therefore be customized to several different operating conditions only by augmenting the controller bank with new controllers.

1.2 Previous work and published literature

Modeling of ice loads and DP systems has been an area of focus for the marine cybernetics group at the NTNU department of marine technology for a few years, and some students have written their project and master thesis on the subject. Stuberg (2009), Røset (2009) and Sørbø (2008) developed methods for modeling of ice resistance in broken ice and level ice. This was used in analyzing vessel response when navigating in ice. The impact of ice in DP operations was also simulated by the students using regular open water DP controllers versus some controllers designed for good performance in ice conditions.

There exists some published work on the problem of DP operations in arctic areas. The major challenges of dynamic positioned vessels in ice-covered waters are discussed by Kuehnlein (2009) and experiences from a few station keeping operations in ice are summarized by Keinonen (2008).

A tutorial on supervisory control theory can be found in the work done by Hespanha (2002). Hespanha et al. (2003) discusses the advantages of logic-based switching over traditional adaptive control. Hybrid control systems for dynamic positioning applications have been studied by Nguyen (2005) who presented a hybrid control system for dynamic positioning control from calm to extreme weather conditions. The problem of bumpless transfer is discussed by Zaccarian & Teel (2002) and Zaccarian & Teel (2001).

This master thesis is an extension of a project thesis by Skogvold (2009) who also discussed a similar topic.

1.3 Contributions

The main contributions of this thesis is the development of a supervisory-switched control system for dynamic positioning of vessels in arctic areas capable of providing satisfactory station keeping in the presence of ice. The work can be summarized as follows:

- Vessel pitch motion in level ice is investigated in a simulation study, model pitch response frequency spectra for level ice and open water conditions are proposed and a method for automatic detection of ice based on spectral analysis of the vessel pitch motion is presented.
- A combined bumpless transfer and anti-windup control scheme based on Zaccarian and Teel (2002) is adapted for use in a DP control system and implemented in the supervisory-switched controller.
- The supervisory-switched DP control system is simulated in a series of tests to assess its performance compared to conventional DP control and to identify the effect of the altering the various parameters in the supervisory control scheme.

1.4 Outline of thesis

Chapter 2 gives the theoretical background and formal definitions of supervisory control, switched systems and bumpless transfer. The chapter is primarily based on Hespanha (2002), Hespanha et al. (2003) and Zaccarian & Teel (2002) and is included to introduce the reader to the concepts of supervisory control.

Chapter 3 gives an overview of different ice regimes and methods to detect ice. The level ice loads on a vessel is investigated through a simulation study with emphasis on detecting dominant load frequencies. The vessel pitch response in open water and level ice conditions is examined in order to detect dominant response frequencies which can be used to detect which operating regime the vessel is in.

Chapter 4 presents the supervisory-switched controller architecture. This includes the design of observers and controllers for use in arctic areas and the supervisor adapted for ice detection based on response frequency spectra.

Chapter 5 contains the results from a simulation study performed to assess the performance of the proposed control system compared to conventional control. A parameter study of the supervisor parameters is also included.

The thesis is concluded in chapter 6 with a summary of the main findings and recommendations for further work.

2 Supervisory control

This chapter is based on work by Hespanha (2002), Hespanha et al. (2003) and Zaccarian & Teel (2002).

Hybrid systems are systems consisting of both continuous time and discrete time components. The supervisory control considered here is a continuous system in connection with either a discrete time (dwell-time) or an event-based switching between controllers for dynamic positioning tailored for different operating regimes. The supervisory control system is supposed to automatically detect which operating regime the vessel is in, and select a suitable controller to use in the feedback loop for the DP control.

Supervisory control can be seen as an adaptive control strategy in the sense that the controller adapts to changes in the system performance by utilizing more than one controller. It can however be argued that it is different from the traditional adaptive control since it can be used to change both the controller parameters and structure. The controller is chosen from a bank of admissible controllers based on a switching logic which evaluates what controller to use in the feedback loop.

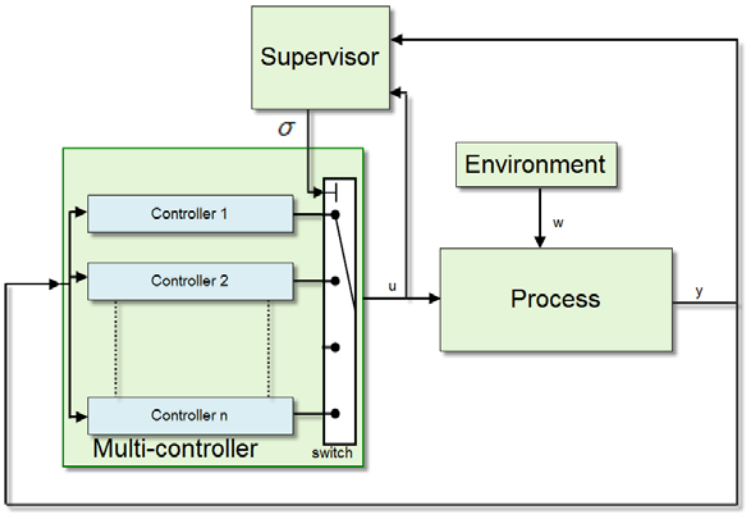

Figure 2 Supervisory control

The purpose of the supervisory control system is to switch among a set of predefined controllers based on measurements collected online. The switching algorithms used for this purpose can be divided into two categories: One can either select which controller to put in the control loop by estimating the model of the process using estimator-based supervision, or one can try to assess the potential performance of every candidate controller directly using performance-based supervision. The switching algorithm considered in this thesis is estimator-based supervision. Figure 2 show the structure of the supervisory control system, where the switching signal, σ, selects what controller to use. In the following, the notation used throughout the thesis is introduced and the components of the supervisory control system is presented.

2.1 Formal definition

Suppose that we want to control the system in a range of operating regimes denoted by the admissible process models in

$$\mathcal{M} \coloneqq \bigcup_{p \in \mathcal{P}} \mathcal{M}_p \tag{2.1}$$

by switching between a bank $\mathcal{C}$ of controllers

$$\mathcal{C} \coloneqq \bigcup_{q \in \mathcal{Q}} \mathcal{C}_q \tag{2.2}$$

where p and q are parameters taking values on the set $\mathcal{P}$ and $\mathcal{Q}$, respectively. For each admissible model in $\mathcal{M}$ there must exist at least one candidate controller in $\mathcal{C}$ that gives satisfactory performance for that admissible model. A controller selection function $\chi : \mathcal{P} \to \mathcal{Q}$ maps each parameter value of $p \in \mathcal{P}$ with the corresponding index $q = \chi(p) \in \mathcal{Q}$ of controller $\mathcal{C}_q$ which provides satisfactory performance when connected to the process model $\mathcal{M}_p$. When the process is believed to be in the model $\mathcal{M}_p$, the controller $\mathcal{C}_q, q \coloneqq \chi(p)$ should be used.

2.2 The switched system

The system resulting from the process, the multi-controller and the multi-estimator is referred to as the *switched system* (Hespanha, 2002), and can be modeled as

$$\dot{\mathbf{x}} = \mathbf{A}_\sigma(\mathbf{x}, \mathbf{w}) \tag{2.3}$$

$$e_p = \mathbf{C}_p(\mathbf{x}, \mathbf{w}), \quad p \in \mathcal{P} \tag{2.4}$$

where $\mathbf{x}$ denotes the state vector of the process, the multi-controller and the multi-estimator, and $\mathbf{w}$ is the vector of environmental disturbances. A_σ and C_p are functions that define the dynamics of the switched system and output functions, respectively. The switched system has a few basic properties; matching property and detectability property.

2.2.1 Matching property

The matching property is a property of the multi-estimator. It means that the set of estimators should be designed such that the output of each process model resembles the actual process output in that particular operating regime. That is, the estimation error e_p is small whenever the actual process is inside the corresponding process model $\mathcal{M}_p$.

2.2.2 Detectability property

The detectability property is a property we impose on the multi-controller. It states that for each fixed estimator, the switched system (2.3)-(2.4) must be detectable with respect to the estimation error e_p when the value of the switching signal is frozen at $\sigma = \chi(p) \in \mathcal{Q}$.

2.3 The supervisor

The supervisor consists of three subsystems: "Multi-estimator", "monitoring signal generator" and a "switching logic". Figure 3 shows the structure of the supervisor using three different process models. Inputs to the supervisor are the process input, u, and measured process states, y. The supervisor output is the switching signal, σ.

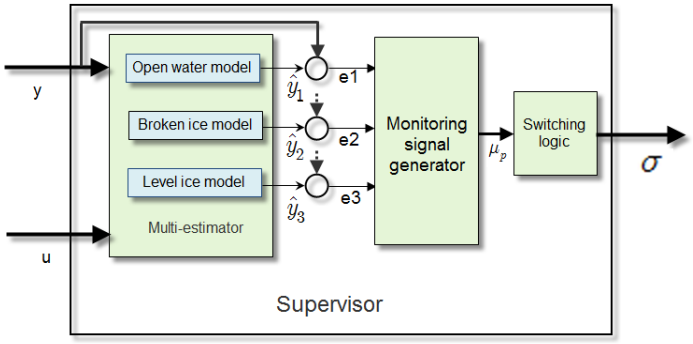

Figure 3 Supervisor components with dynamical systems

2.3.1 Multi-estimator

The estimator-based supervisory control uses a multi-estimator containing several models of different operating regimes for the process. Typically, the multi-estimator is a dynamical system consisting of differential equations for each process model, but may also be based on other models of the process such as the model frequency spectra described in section 3.1.3. In the case of DP systems in ice, the multi-estimator should consist of models of the ship in open water in addition to models of different ice conditions.

2.3.2 Monitoring signal

The "goodness" of each model in the supervisor is monitored by the use of a monitoring signal, μ which compares the performance of the different models. By using a monitoring signal to assess the performance of the models instead of directly comparing the model estimate errors, the signal can be filtered to reduce the effect of noise etc. The monitoring signal also allows the designer to manipulate the signal such that one model is more sensitive to changes on estimate errors than another, i.e. the monitoring signal corresponding to one model may be more susceptible to changes in estimate error. The monitoring signal should be based on some integral norm of the error between process output and the estimates for each model. Hespanha (2002) defines the following monitoring signal:

$$\mu_p(t) = \epsilon + e^{-\lambda t}\epsilon_0 + \int_0^t e^{-\lambda(t-\tau)}\gamma_p(\|e_p(\tau)\|)d\tau, \quad p \in \mathcal{P} \tag{2.5}$$

where ϵ and ϵ_0 are non-negative constants with at least one of them strictly positive, λ is a non-negative forgetting factor, γ_p is a class κ [1] function, $\|\bullet\|$ is any vector norm and $e_p = y_p - y$ is the error between model estimate p and measurements from the actual process.

The monitoring signal may be generated by the following dynamical system

$$\dot{\mu}_p = -\lambda\mu_p + \gamma_p(\|e_p\|), \quad p \in \mathcal{P} \tag{2.6}$$

2.3.3 Switching

The switching between controllers in the controller bank is orchestrated by a switching logic. The switching logic takes the monitoring signal as input and decides which controller to use in the control loop. A small monitoring signal suggest that the actual process lies near the corresponding process model, and hence a controller designed for that operating regime should be put in the control loop. We will here look at two different switching logic algorithms and explain their applicability to arctic DP systems.

Dwell-time switching logic

One way to solve the switching task is to evaluate the controller performance periodically and then switch to the best suitable controller based on the smallness of the error between the estimated and the measured state vector. To always have the best possible controller in the loop, one might want to evaluate the controller performance continuously, but this could lead to very fast switching between controllers. Even though we are only switching between stable controllers, too fast switching may lead to an unstable system (Hespanha, 2002). The problem of fast switching is called chattering and can be avoided if we "dwell" at the selected controller for some time before the controller performance is evaluated again. By doing this, the switching is slowed down, and by choosing the "dwell time" for the switching logic, we can make sure that the total system stays stable. Figure 4 explains the concept.

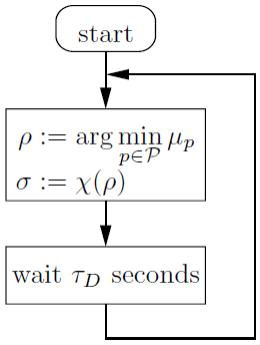

Figure 4 dwell-time switching logic (Hespanha, 2002)

[1] A continuous function $\alpha : [0, a) \to [0, \infty)$ is said to belong to class κ if it is strictly increasing and $\alpha(0) = 0$. (Khalil, 2002)

Scale-independent hysteresis switching logic

When using the dwell-time switching logic, the performance of the controller can be significantly worsened during the “dwell time”. It could therefore be interesting to investigate other switching logics. Hespanha (1998) introduced the scale-independent hysteresis switching logic which continuously searches for the process model which gives the minimum error from the measured states. It solves the problem of chattering by slowing down the switching using a hysteresis switching logic. As shown in Figure 5, the performance of each admissible process model is continuously evaluated.

By requiring the monitoring signal of the "best" process model to be strictly less than the monitoring signal of the process currently in the loop before switching, chattering can be avoided. The hysteresis constant, h, decides how fast the switching is allowed to happen.

Two properties needs to be satisfied by the monitoring signal generator and the switching signal: The small error property and the non-destabilization property.

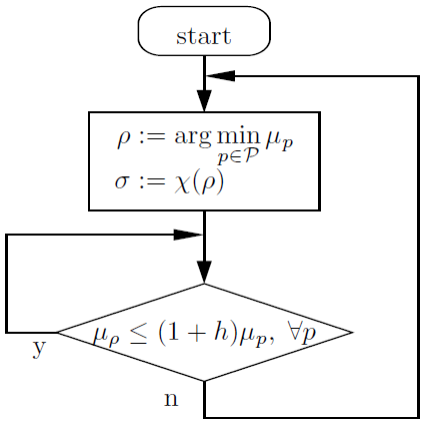

Figure 5 Scale-independent hysteresis switching logic (Hespanha, 2002)

2.3.4 Small error property

The small error property means that there is a bound on e_ρ in terms of the smallest signal e_p for a process switching signal for which $\sigma = \chi(\rho)$. For example for the scale-independent hysteresis switching with the monitoring signal in (2.6) we have

$$\int_0^t e^{-\lambda(t-\tau)}\gamma_\rho(\|e_\rho(\tau)\|)d\tau \leq (1+h)m\mu_p(t), \quad \forall t > 0, \forall p \in \mathcal{P} \tag{2.7}$$

where $\mathcal{P}$ is a finite set with m elements (Hespanha, 2002)

2.3.5 Non-destabilization property

The switching signal σ has the non-destabilization property if it preserves the detectability property in a time-varying sense, i.e., if the switched system (2.3)-(2.4) is detectable with respect to the switched output e_ρ, for a process switching signal ρ and with $\sigma = \chi(\rho)$. This property holds if the switching stops

in a finite time which is the case of the scale-independent hysteresis switching logic or if the switching is slow on the average which can be achieved by the dwell-time switching logic.

For the scale-independent hysteresis switching logic and monitoring signal (2.6) we have that

$$N_\sigma(\tau,t) \leq 1 + m + \frac{m \log\left(\frac{\mu_p(t)}{\epsilon + e^{-\lambda t}\epsilon_0}\right)}{\log(1+h)} + \frac{m\lambda(t-\tau)}{\log(1+h)}, \quad \forall t > \tau \geq 0, \forall p \in \mathcal{P} \tag{2.8}$$

where $N_\sigma(\tau,t)$ is the number of discontinuities (switching events) of the switching signal σ in the open interval (τ,t) (Hespanha, 2002). We see that increasing the hysteresis constant h, reduces the number of discontinuities while increasing the forgetting factor λ, increases the number of discontinuities.

2.4 Bumpless transfer

When performing switching between the controllers in the controller bank, the different controllers may have very different commanded control force as their output at the switching instants. If the switching is performed without giving this problem a thought, it may lead to sudden changes in the command signal to the actuators (thrusters). As the thrusters has some physical constraints, they will not be able to follow the commanded signal if the signal has a discontinuity. To ensure that the controller will not command too excessive command signals one should correct the commanded signal such that unwanted transients will not occur after a switching instant. The thrusters will also experience increased wear and tear due to these rapid changes in set point. To cope with these problems, bumpless transfer between the controllers should be implemented in a supervisory control system.

A problem closely related to the bumpless transfer problem, is the anti-windup problem which occurs due to actuator saturation combined with slow controller dynamics such as integrator action. The two problems can be solved using similar techniques. This section will present a solution to both the bumpless transfer problem and the anti-windup problem scheme proposed by Zaccarian & Teel (2002) and show how this can be applied to the case of a supervisory-switched DP system.

2.4.1 Concept

Figure 6 shows a block diagram of the model-based bumpless transfer control scheme (Zaccarian & Teel, 2002). We see that each bumpless transfer block ($\mathcal{AW}_q$) takes the difference of the actual actuator action and the calculated control signal from controller $\mathcal{C}_q$ as input and use this to adjust both the reference input to the controller and the actuator control signal.

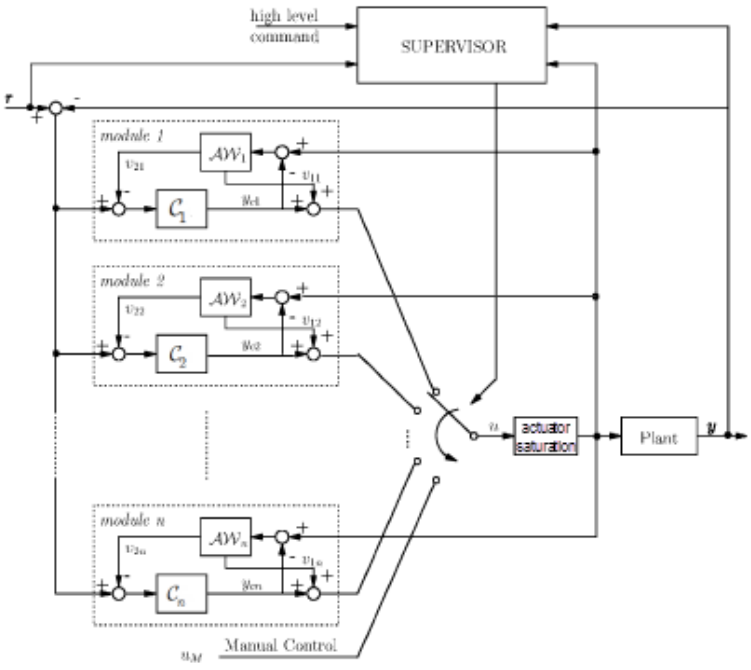

Figure 6 Bumpless transfer scheme (based on Zaccarian & Teel (2002))

The dynamics of the q'th module is given by

$$\dot{\xi}_q = A\xi_q + B(sat(u) - y_{cq}) \tag{2.9}$$

$$v_{1q} = K_q\xi_q + L_q(sat(u) - y_{cq}) \tag{2.10}$$

$$v_{2q} = -C\xi_q - D(sat(u) - y_{cq}) \tag{2.11}$$

$$y_{cq} = \mathcal{C}_q(r - y - v_{2q}) \tag{2.12}$$

where A and B are the system matrix and control matrix, respectively, of the controlled plant, ξ is the state vector for the bumpless transfer block, K_q and L_q are design matrices to be selected. $\mathcal{C}_q$ is the q'th controller in the controller bank and $sat(u)$ is the actuator output where saturation have been accounted for. y_{cq} is the output of controller q, r is the reference command to the controller and y is the plant measurements. Finally, the controller command signal is given by

$$u = y_{c\sigma} + v_{1\sigma} \tag{2.13}$$

where σ denotes which controller is currently connected to the system

2.4.2 Implementation issues

A and B_2 should represent the most important dynamics of the ship. Sørensen (2005) presents a simplified model of the ship for use in model-based control, called the control plant model. This model is given as

$$\dot{\eta} = R(\psi)\nu \tag{2.14}$$

$$M\dot{\nu} = -D\nu + \tau_c + w \tag{2.15}$$

where

$$R(\psi) = \begin{bmatrix} \cos\psi & -\sin\psi & 0 \\ \sin\psi & \cos\psi & 0 \\ 0 & 0 & 1 \end{bmatrix} \tag{2.16}$$

is the rotation matrix between the body-fixed velocity vector, ν and the earth-fixed position vector, η. τ_c is the vector of actuator forces on the vessel and w is the vector of environmental disturbances acting on the vessel. The control plant model (2.14)-(2.15) is nonlinear because of the rotation matrix. We want to define a state-space realization of the control plant model for use in the bumpless transfer scheme. Rewriting the control plant model as

$$\begin{bmatrix} \dot{\eta} \\ \dot{\nu} \end{bmatrix} = \begin{bmatrix} 0 & R(\psi) \\ 0 & -M^{-1}D \end{bmatrix} \begin{bmatrix} \eta \\ \nu \end{bmatrix} + \begin{bmatrix} 0 \\ M^{-1} \end{bmatrix} \tau_c + \begin{bmatrix} 0 \\ M^{-1} \end{bmatrix} d \tag{2.17}$$

and defining the state vector as $\xi = \begin{bmatrix} \eta & \nu \end{bmatrix}^T$ and the control input as $u = \tau$ we can write the control plant model on state-space form:

$$\dot{\xi} = A(\psi)\xi + Bu = \begin{bmatrix} A_1(\psi) \\ A_2 \end{bmatrix} \xi + B_1 u + B_2 d \tag{2.18}$$

where the system matrix have been divided into a nonlinear and linear part, $A_1 = \begin{bmatrix} 0 & R(\psi) \end{bmatrix}$ and $A_2 = \begin{bmatrix} 0 & -M^{-1}D \end{bmatrix}$, respectively. To analyze the system and for synthesis of the gains in the bumpless transfer scheme one could linearize the system matrix around several heading angles and check that all of the linearized system matrices satisfy the conditions following conditions:

"Suppose each of the linear (unsaturated) closed-loop interconnections is internally stable. If there exists $P = P^T > 0$, $W = W^T > 0$ *(diagonal) such that*

$$\begin{bmatrix} A^T + PA & PB_2 + {K_q}^T W \\ (PB_2 + {K_q}^T W)^T & {L_q}^T W + W L_q - 2W \end{bmatrix} < 0 \quad \forall q \in \mathcal{Q} \tag{2.19}$$

then, for any switching strategy, the bumpless transfer scheme is well posed and guarantees $\mathcal{L}_p$ *stability from* (w,r) *to the overall system state for all* $p \in [1,\infty]$*." (Zaccarian & Teel, 2002)*

2.4.3 Gain calculation by LMIs

Condition (2.19) can be rewritten as a Linear Matrix Inequality (LMI) which can be solved to find L_q and K_q using available software[2]. Since all of the bumpless transfer modules have the same dynamics, all of the L_q K_q can be taken to be the same. Rewriting condition (2.19) with $Q \coloneqq P^{-1}$, $U \coloneqq W^{-1}$, $X_1 \coloneqq KQ$ and $X_2 \coloneqq LU$ we arrive at

$$\begin{bmatrix} QA^T + AQ & B_2U + X_1^T \\ UB_2^T + X_1 & X_2^T + X_2 - 2U \end{bmatrix} < 0 \tag{2.20}$$

By defining one LMI constraint for each of the linearized system matrices, we can solve the problem and find suitable bumpless transfer gains which satisfies all of the constraints and are valid for all operating headings. From the solution of these LMI's we find the gains as $K = X_1Q^{-1}$ and $L = X_2U^{-1}$

[2] For example Yalmip (Löfberg, 2004) with SeDuMi solver for MATLAB

3 Ice

Sea ice can be divided into four types:

- Broken ice is ice consisting of relatively small ice floes broken off from the sea cover. It is the typical ice type encountered at the transition between open water and level ice or in ice breaker channels (managed ice).
- Level ice is a large ice cover of uniform thickness. It can range from 10 cm to a couple of meters thickness. To pass through the level ice, the ice needs to be broken by an ice breaking bow.
- Ice ridges are thick ridges formed by two colliding ice sheets and can be up to 30 meters deep. The ice ridges may require several attempts to break through, or it may not be possible to break through, depending on the deepness and size of the ridge.
- The most severe ice conditions involve ice bergs. These are massive pieces of ice collections of multi-year ice which have broken away from a glacier. The ice bergs may be afloat or aground and are generally not possible to break through with ships.

The actual ice conditions are normally combinations of some of these ice types.

In this chapter, various methods for ice detection is reviewed, and a method for detection of operating regime based on spectral analysis of vessel pitch motion measurements is presented through a simulation study of the vessel in open water and level ice.

3.1 Ice detection

One of the main challenges with the supervisory control is to detect what operating regime the ship is operating in, i.e. if it is sailing in open water, broken ice, level ice, etc. To detect this, one can use different procedures such as various ice detection sensors or a model of the vessel motion in the different operating regimes.

3.1.1 Sensors

Radar

A marine radar is normally installed in all ships. The radar is used to navigate in bad weather or in the dark and enables the captain to see objects far away or in bad visibility. In its standard version, the radar can detect large ice formations such as icebergs. It can, however, be modified to enable it to detect other types of ice. This is the topic of Lewis et al. (1987), where a radar system optimized for ice detection is presented. The system can be used for both open-water detection of icebergs and classification of ice types (distinguishing between first-year, multi-year and ridged ice) for the purpose of close-tactical maneuvering.

A more accurate technique is side-looking radar (SLR) and synthetic aperture radar (SAR). Aircraft-mounted SLR and SAR were used extensively until the 1980s for ice detection and classification (Sandven & Johannessen, 2006). From an operational point of view, the airborne radar has a number of drawbacks including the fact that the aircraft will most likely not be able to continuously overfly the vessel and the solution is relatively costly. The airplane will also be dependent on a nearby airport to be

stationed at. Today, the SLR and SAR monitoring techniques are mostly used in space borne sea ice monitoring systems.

Satellite

Satellite surveillance is the most common method for remote sensing of sea ice today. Several countries provide ice charts which are updated daily throughout the ice-season. These charts are based largely on satellite borne detection devices. In addition to the satellite mounted radars (SLR and SAR) there have been some development of a new generation of microwave radiometers which can provide images with high resolution (Sandven & Johannessen, 2006).

None of these methods are optimal for close-tactics maneuvering and DP operations as they have limitations with regards to the resolution of the satellite images. Even though the images sometimes can be accessed near real-time, they are still of a discrete nature and normally have some time delay from the images are captured until they can be used onboard the vessel. The satellite images are, however, very useful for more long-term planning of marine operations or choice of sailing route.

Visual observation

Visual observation of ice conditions is maybe the most reliable and easiest method of ice detection and classification. At least for the separation of open water conditions and full ice coverage conditions in clear daylight, this is a trivial task. By continuously monitoring the area around the vessel the captain can detect the ice and choose to shut down the operation if the ice conditions are too severe for safe operation or take actions as required to ensure continued operation. These actions include adjustments in the DP control system.

The visual ice detection can be difficult if the visibility is bad. It is also very difficult to separate the different ice regimes only by visual observation of the ice surface. In Figure 7 we can see a typical ice condition consisting of different ice regimes. It is not difficult to imagine that it could be hard to separate the level ice, broken (managed) ice and ice ridges from each other only by visual observation.

Figure 7 Visual observation of ice conditions

Since it under normal conditions is possible to detect the transition from open water to level ice by visual observation, the supervisory control system considered in this thesis can therefore be seen as a safety system where the DP system automatically adjusts to the changing conditions when the ice hits the vessel if this is not done ahead of the ice impact.

Hull vibrations

When the vessel enters an ice regime the high-frequency ice breaking and ice crushing loads will induce vibrations in the hull. This will also be noticed as a rumble sound inside the ship. It may be possible to detect the vibrations by inertial measurement. Through signal processing of the vibration measurements one may also be able to detect which ice regime the vessel is sailing in.

3.1.2 Dynamic models

In the supervisory control context, the typical methods for detection of operating regime is to develop a dynamic model of each admissible process and compare the actual process measurements with the output of the process models. This is however dependent on accurate and reliable models for the operation in all of the regimes. There are developed very good models of the ship in open water using observer design (for example the non-linear passive observer presented in section 4.1.1), but the influence of ice is not easily implemented in detail in these models.

Skogvold (2009) used an open water observer modified with more aggressive tuning of observer bias estimation gains and time constants for use as ice process models. This gave good detection of the points where the vessel entered and exited ice regimes, but the method was not very robust as the bias estimation of the open water observer regained the open water model as the best fit after a while even if the vessel was still in an ice regime. This feature can be thought of as what is referred to as the term "weak detectability" in the fault diagnosis and control literature (Blanke et al., 2006). Although this may be OK in terms of controlling the vessel (the open water integrator gain may have had time to integrate

up the ice disturbances), it is not desirable in terms of having the choice to keep the same controller throughout an ice regime.

3.1.3 Spectral analysis

Instead of looking at the dynamics of the different process models, we can look at the frequency spectrum of the vessel motion. It is expected that the frequency response spectrum of open water compared to ice conditions shows clear differences. The detection based on spectral analysis is motivated by Nguyen (2005) where a similar procedure was used to detect the peak frequency of the sea state based on surge, sway and yaw response of the vessel.

When operating in open water with waves, the surge, sway and yaw motions are very much influenced by the wave motion since these are usually filtered out from the control algorithm and not counteracted by the DP system. This is not the case for operation in ice covered waters. The surge, sway and yaw motions due to ice loads should not be filtered out, and should be counteracted by the control system. The frequency spectrum in these degrees of freedom will therefore be very influenced by what controller is currently in the feedback loop. The motions will also have a low frequency character which means that one would have to buffer the position signal for quite a while before the motions are captured by the spectral analysis with sufficient accuracy.

By measuring the pitch motion of the vessel with a motion reference unit (MRU), these motions may be used to detect which regime the vessel is operating in. The pitch, roll and heave motions are usually not controlled in DP systems for ships, and they will therefore not be affected by the controller in the same degree as the three horizontal motions. The pitch motion of the vessel is also more susceptible to loads of higher frequency than the surge, sway and yaw motion. These frequencies are captured by the spectral analysis with sufficient accuracy even with relatively short signal buffer time.

3.2 Level ice

The ice forces a vessel experiences when it encounters a level ice regime, are characterized by a combination of crushing loads, ice bending loads and ice submersion loads. An ice breaking event is a cycle of crushing and bending. The bending loads and ice submersion loads can be considered as slowly-varying forces (Røset, 2009). The crushing forces appear as "spikes" in the ice loads when the bow hits the ice and causes a piece of the ice to break off.

The ice-breaking occurs each time the vessel bow has penetrated a certain distance into the ice and the weight of the bow on the ice sheet causes the ice to fracture. When the ice has a constant speed towards the vessel, this ice-breaking is expected to act as a periodic force where the period of ice breaking is a function of the relative velocity between the vessel and the level ice. This hypothesis will be tested in a simulation study.

3.2.1 Level ice load frequencies

A small simulation study in MCSim of a vessel in level ice is performed to study the level ice forces, and to explore possible techniques to detect when a vessel hits level ice without the use of ice measurements. One idea is, as explained above, to look at the vessel response in level ice in the frequency plane to detect the most dominating vessel response frequencies in level ice. In the following,

level ice forces and vessel response will be studied in time- and frequency domain. The level ice forces are calculated using a 6DOF algorithm developed by Røset (2009). Special attention is on whether certain response frequencies can give information about the ice properties which can be used in the control strategy. This simulation also serves as a validation of the ice force calculation algorithm.

The simulation will look at the ice forces when the vessel hits the ice head on while performing station keeping. While the main focus of the simulation is to identify the nature of the ice forces, and not on the DP performance, a DP controller using feedforward of the ice forces will be used. The calculated control forces will also be fed back to the vessel without any time delay or other thruster dynamic influence. This way, we can assume that the vessel is capable to perform station keeping without large deviations from the desired position.

The vessel used in the simulation study is the MC Supply in the MCSim simulator, whose dimensions are given in Table 1.

MC Supply	
Length	80 [m]
Breadth	17.4 [m]
Draft	5.6 [m]
Displacement	6000 [m^3]
Bow stem angle	24°
Side stem angle	90°

Table 1 MC Supply dimensions

Simulation with different ice drift velocities will be investigated:

1. Slow drift: $V_{ice} = 0.01[m/s]$
2. Normal drift: $V_{ice} = 0.3 - 0.5 - 0.7[m/s]$
3. Fast drift: $V_{ice} = 3.0[m/s]$

Ice condition used in the simulation study is given in Table 2. In addition to the ice loads, the environmental conditions include a current with the same direction and velocity as the drifting ice.

Ice conditions	
Ice regime	Level ice
Compressive strength	$5 \cdot 10^6$ [Pa]
Flexural strength	$6 \cdot 10^5$ [Pa]
Ice thickness	0.5 [m]
Young's modulus	$5.4 \cdot 10^9$ [Pa]

Table 2 Level ice conditions

Slow drift simulation

This simulation is performed to learn more about the ice loads and the vessel response in each single ice breaking event. The ice drifts towards the vessel very slowly, and the transient effects of the vessel

response dies out before the next breaking event happens. Figure 8 shows the ice loads in pitch as well as the vessel pitch response throughout the entire simulation (0s-10000s).

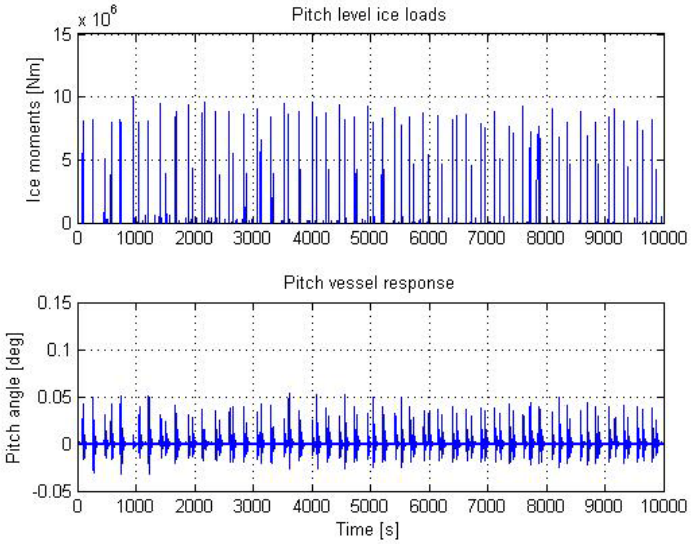

Figure 8 Pitch level ice loads and vessel response

Focusing on the ice loads, we can see that there are clear peaks in the load plot due to the ice breaking as well as some smaller peaks from the ice crushing between breaking events. We see that each breaking event cause the vessel to oscillate with a small amplitude around zero degrees.

To understand the nature of the ice loads and the vessel response better, a Fast Fourier Transform (FFT) of the signals is performed. The resulting ice load and vessel response frequency spectra can be seen in the upper and lower part, respectively, of Figure 9.

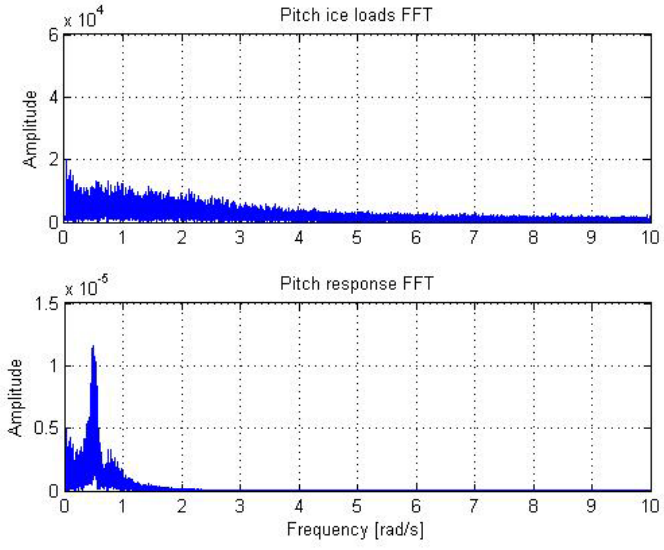

Figure 9 Pitch ice loads and vessel response frequency spectra

The ice loads frequency spectrum does not have a distinct peak frequency, and the load spectrum seems to be of a noisy character dominated by frequencies in the lower range. This corresponds well to the findings of Bjerkås et al (2007), where ice loads against a lighthouse was investigated.

The vessel response frequency spectrum shows that the vessel acts as a low-pass filter due to its large mass. Only response frequencies up to approximately 2 [rad/s] can be noticed in the response spectrum. Loads of higher frequency than this will not affect the vessel motion, but may be noticed as high-frequency vibrations in the hull. In contrast to the noisy ice load spectrum, the vessel response frequency spectrum does show a clear peak frequency at 0.5 [rad/s]. When the vessel is excited by a load which has energy evenly distributed over the frequency spectrum, it will oscillate with the vessel natural frequency. The peak in the vessel response frequency spectrum corresponds to the natural frequency in pitch.

To see the response of each breaking event more clearly, we show a zoom-in (5000s-5500s) of the loads and response in Figure 10.

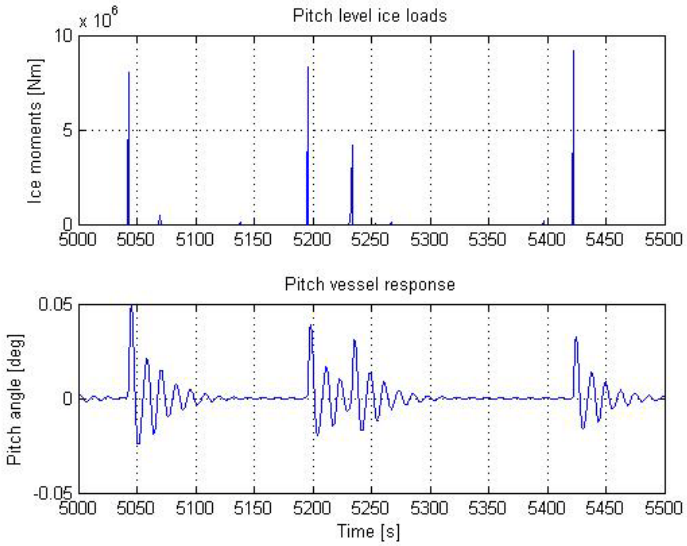

Figure 10 Pitch level ice loads and vessel response zoom-in

This figure also confirms that the natural period of the vessel in pitch is 0.5 [rad/s]. After the impulse load at 5040 seconds, the vessel oscillates 5 times in ca. 60 seconds. Hence, an estimate of the natural frequency in pitch can be calculated as

$$\omega_{0,5} \approx \frac{5}{60[s]} \cdot 2\pi[rad] \approx 0.50[rad/s] \tag{3.1}$$

Medium and fast drift simulation

A simulation of the vessel-ice interaction where the ice drift velocity is increased to 0.3 [m/s] is performed to capture the vessel response to a continuous ice loading condition where the vessel response does not go back to its equilibrium position between ice breaking events. This is a more

"normal" ice drift velocity and is considered to be a likely drift velocity for a drifting level ice sheet. Again, we focus on the pitch motion and the ice loads. Figure 11 shows the pitch ice loads and vessel motion time series.

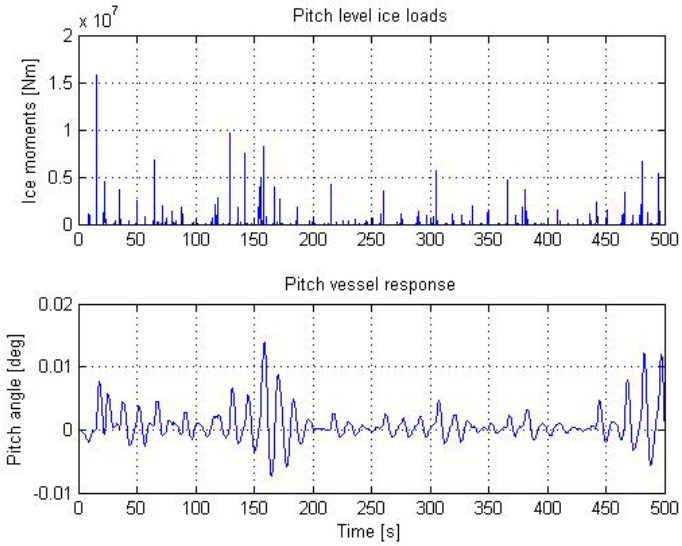

Figure 11 Pitch level ice loads (top) and vessel response (bottom) for 0.3 m/s drift velocity

As expected, the load time series shows that the ice breaking is more frequent when the drift velocity of the ice is increased to 0.3 [m/s]. This causes the vessel pitch motion to be affected by the previous breaking events, and the bow is above the ice sheet much of the time. To evaluate the loads and vessel motion, we perform an FFT analysis on the signals again. The frequency spectra are shown in Figure 12.

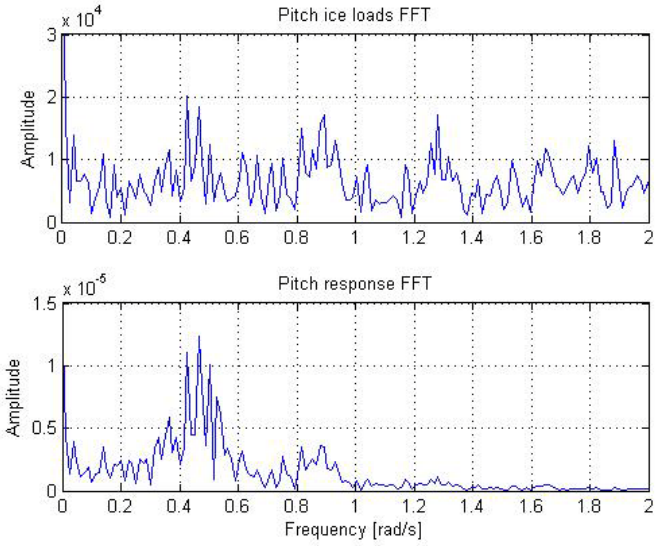

Figure 12 Pitch ice loads spectrum (top) and vessel response frequency spectrum (bottom) for 0.3 m/s drift velocity

Again, we see the same features of the frequency spectra as for the slow drift case: The noisy ice loads, the low-pass effect on the vessel motion and a peak at the vessel natural frequency. In addition to this,

we see that the ice load and response spectra shows a large amplitude at zero frequency. This is because the bow of the vessel is pushed on top of the ice sheet much of the time due to the drifting ice. This feature of the motion spectrum can be used to detect that the vessel is in a level ice condition. We can also observe a small peak in both spectra around 0.9 [rad/s]. One may think that this is a result of the ice breaking frequency which would corresponds to an ice break period,

$$T_{icebreak} = \frac{2\pi[rad]}{0.9[rad\ /\ s]} \approx 7[s] \tag{3.2}$$

To examine this hypothesis, several simulations with different ice drift velocity are performed to see if it is possible to track this frequency peak. The load and response spectra for 0.5 and 0.7 [m/s] drift velocities are shown in Figure 13 and Figure 14, respectively.

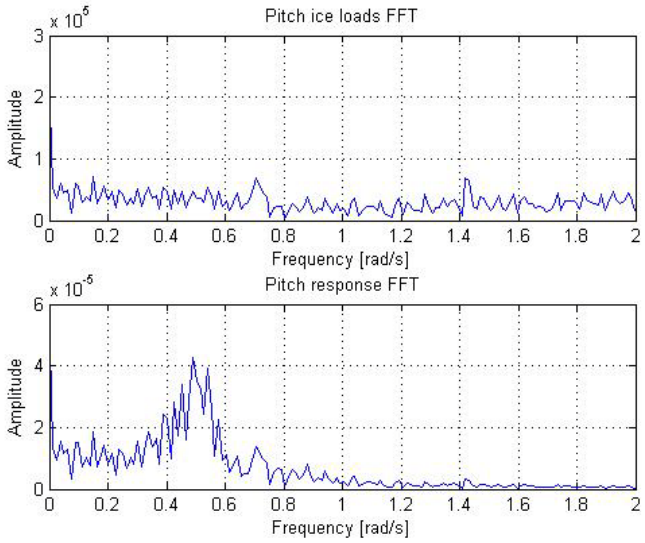

Figure 13 Pitch ice loads spectrum (top) and vessel response frequency spectrum (bottom) for 0.5 m/s drift velocity

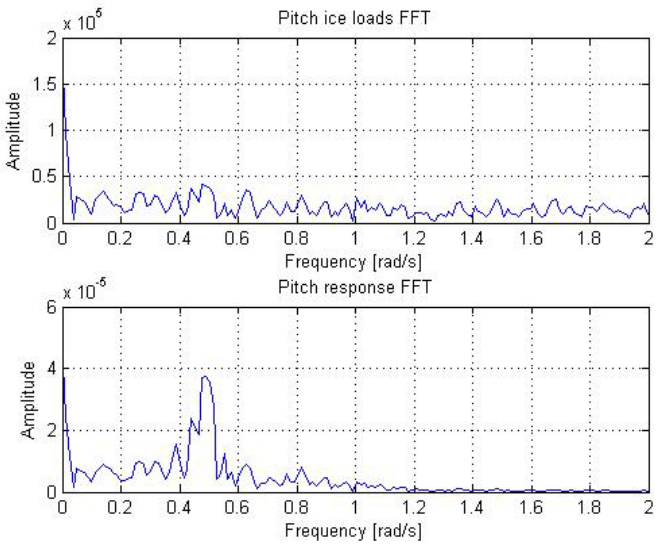

Figure 14 Ice pitch ice loads spectrum (top) and vessel response frequency spectrum (bottom) for 0.7 m/s drift velocity

It is difficult to conclude with anything regarding the breaking frequency from these simulations, all the time we cannot track any clear peaks in the frequency spectrum other than the normal frequency and the peak at zero rad/s. The small peaks we noticed other than these two frequencies are probably more or less random as they do not seem to follow the expected behavior when the drift velocity is altered.

To take the ice model to the extreme, a test with ice drift velocity of 3 [m/s] is performed. This is not considered as a realistic scenario, but is included to see if there can be observed a speed-dependant ice breaking frequency in either the load spectrum or the motion spectrum of the vessel. This simulation did not show a clear peak resulting from ice breaking either. The pitch response spectrum is shown in Figure 15.

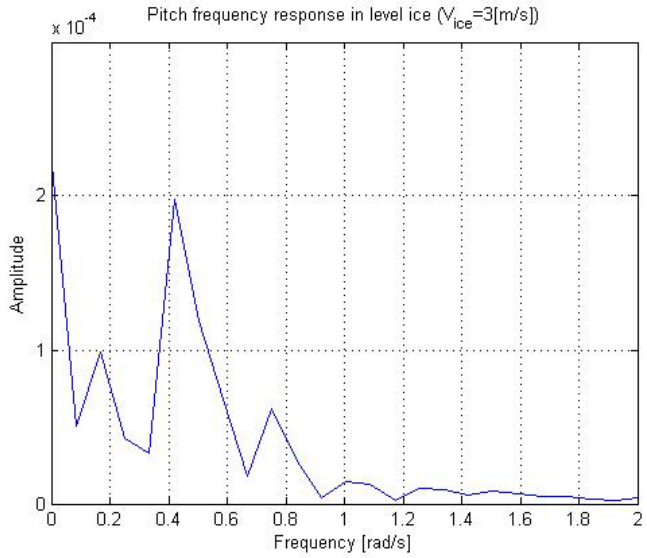

Figure 15 Pitch response frequency spectrum for fast ice drift

There may be several reasons to why we are not able to detect the ice breaking frequency in neither the load spectrum nor the response spectrum. The ice breaking is not necessarily a "clean" periodic load, i.e. the peak in the load frequency spectrum is very wide and not easily recognizable in the spectrum. Another reason may be that the algorithm for calculation of the level ice loads does not give realistic ice loads. One issue in particular, is that the response angles due to ice loading seems to be very small. Perhaps the level ice algorithm underestimates the pitch loads. This is however an area for further investigation and the level ice algorithm is used throughout the thesis without further actions on this area.

3.2.2 Proposed level ice frequency model

The simulations showed that the vessel pitch motion in level ice was characterized by to clear peaks in the frequency spectrum; one at zero and one at the natural frequency of the vessel. The simulations did not show any clear connection between ice drift velocity and vessel response. The proposed frequency model for level ice condition can therefore be based solely as a function of vessel natural frequency. In practice, the pitch natural frequency is usually known for every vessel and can thus be used to generate model frequency spectra for use in the ice detection process.

One difference we saw from the simulations was that the amplitude of the frequency spectrum varied somewhat between the various drift velocities. To be able to compare the frequency spectra in the supervisor regardless of ice drift speed, the level ice frequency model spectrum is normalized to a unit length.

A formula which can be used to generate the frequency model can be based upon a curve fitting of the frequency spectra using a sum of Gaussian peaks. A Gaussian peak has the fundamental functional form

$$f(x) = a\exp\left[-\frac{1}{2}\left(\frac{x-b}{c}\right)^2\right] \tag{3.3}$$

where the parameter a is the height of the peak, b is the position of the peak and c is related to the width of the peak.

Thus, the two characteristic peaks of the level ice spectrum can be represented by a sum of two Gaussian peaks where the parameters can be estimated from known frequency spectra using curve fitting techniques. One example of frequency model, is

$$S_{LevelIce}(\omega) = 0.3731\exp\left[-\left(\frac{\omega}{0.042}\right)^2\right] + 0.2278\exp\left[-\left(\frac{\omega-0.5}{0.1234}\right)^2\right] \tag{3.4}$$

where the a and c parameters in (3.3) have been selected with use of Matlab's curve fitting toolbox on the response frequency spectrum in Figure 11. The position of the peaks (parameter b) is chosen as the observed peaks at zero and normal frequency. The normalized response spectrum and the approximation (3.4) is shown together in Figure 16.

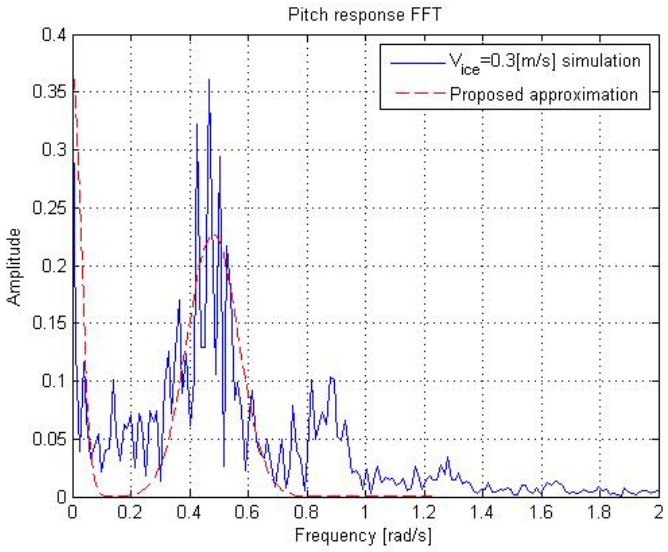

Figure 16 Proposed level ice pitch frequency model

3.3 Broken Ice

The MCSim broken ice module is currently modeled only in the 3 horizontal degrees of freedom and hence does not include forces in pitch. It will therefore not be considered any further in this thesis. In real life though, it would probably be possible to separate the pitch frequency response in broken ice from level ice.

3.4 Open water

3.4.1 Pitch frequency response in waves

The frequency response of the vessel in open water is greatly affected by the wave conditions. The peak frequency of the response spectrum is normally located close to the dominating wave frequency. Depending on the distribution of wave frequencies, the response spectrum may have a single, clear peak frequency. Figure 17 shows an example of the vessel response in waves generated according to the Jonswap wave spectrum with environmental conditions as shown in Figure 17. The wind velocity is chosen somewhat higher than the expectation value based on significant waves height (5.19 [m/s]) since the Jonswap spectrum is developed for conditions in the North Sea whereas the influence of ice close to the vessel will reduce the wind fetch distance compared to the theory behind the Jonswap spectrum.

Environmental loads	
Significant wave height	1.0 [m]
Mean wave direction	180° (bow)
Mean wind velocity	8.0 [m/s]
Mean wind direction	180°
Current velocity	0.3 [m/s]
Current direction	180°

Table 3 Environmental conditions for open water with waves

The vessel response also shown this same peak frequency. In contrast to the level ice frequency response spectrum, there is almost zero amplitude at zero frequency relative to the amplitude at the peak frequency. This is because the vessel only oscillates around zero pitch angle.

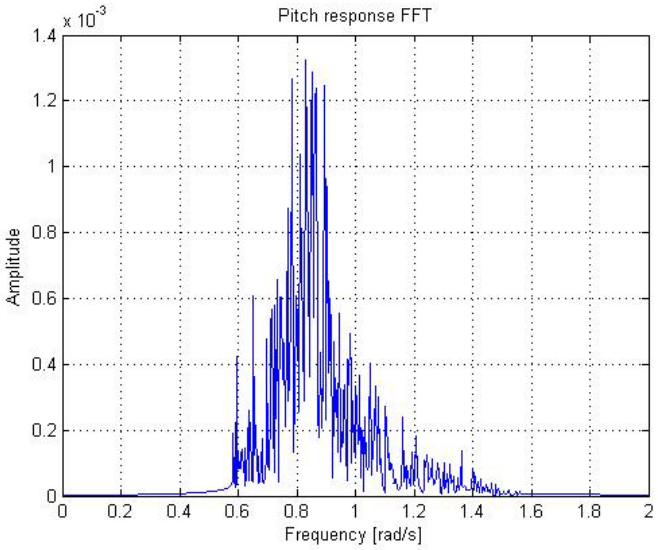

Figure 17 Open water pitch response

Studying the frequency response spectra presented above, we can see a clear difference between the open water and level ice case. In the example simulations shown here, the influence of waves makes the separation of the two regimes (open water and level ice) very easy. If there were no waves outside the ice regime, or there were some wave movement in the ice, the difference would not be as clear, but it should still be possible to detect the characteristics of the level ice response spectrum (peak at zero and natural frequency). The situation which is expected to cause pitch motion with a frequency spectrum that could resemble the level ice spectrum is environmental conditions involving a current but no waves. A simulation with environmental conditions as shown in Table 4 is therefore performed to investigate the resulting motion spectrum.

Environmental loads	
Significant wave height	- [m]
Mean wave direction	-
Mean wind velocity	- [m/s]
Mean wind direction	-
Current velocity	0.3 [m/s]
Current direction	180° (bow)

Table 4 Current simulation environmental conditions

The pitch motion and its frequency spectrum is shown in Figure 18. This spectrum is not similar to the proposed level ice frequency spectrum model, and it should be possible to separate the two conditions from each other by using the proposed spectral analysis of the pitch motion in the supervisory control system.

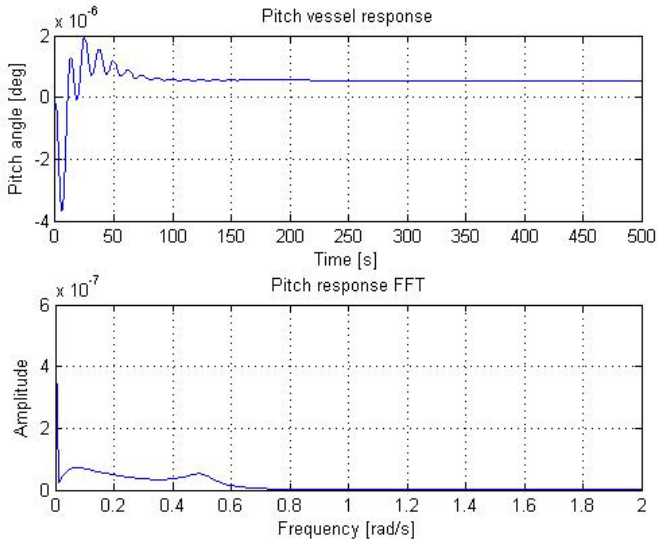

Figure 18 Pitch motion time series (top) and FFT (bottom) for open water simulation without waves

One would maybe need to add a model of the open water condition with no waves to the bank of admissible models to be sure that the situation without waves is not confused with the level ice case. This is however not considered any further in this thesis, and the open water frequency model spectrum is approximated by a single Gaussian peak at the position of the most dominant wave frequency. An important remark to make is that the wave frequency and the vessel response frequency is not the same. The vessel response comes from a series of signal transformations from wave motion through wave loads to vessel response. To get the most accurate response spectrum model, one should include the RAO data[3] of the vessel subject to waves for varying frequencies. The assumption that the peak response frequency is close to the peak wave frequency is however valid for most cases (Sørensen, 2005). The proposed open water frequency spectrum is therefore approximated by

$$S_{OpenWater}(\omega) = 0.1189 \exp\left[-\left(\frac{\omega - \omega_{peak}}{0.1433}\right)^2\right] \tag{3.5}$$

where the amplitude and peak width parameters have been found using the Matlab curve fitting tool on the normalized version of the simulated frequency response spectrum in Figure 17. The normalized spectrum and the proposed open water model spectrum for $\omega_{peak} = 0.8308$ is shown in Figure 19.The dominating wave frequency would have to be estimated (for example from wind measurements) or measured by wave sensors.

[3] Response amplitude operator (RAO) data may be calculated using a numerical ships motion program such as ShipX VERES.

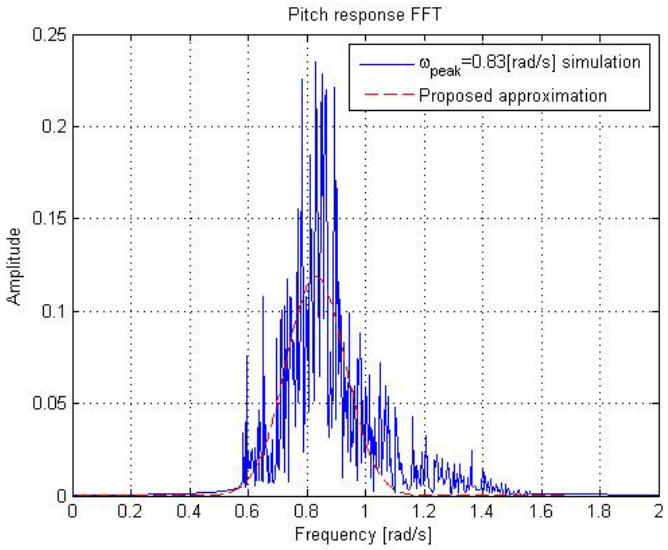

Figure 19 Proposed open water pitch frequency model

4 Supervisory-switched DP control system design

A marine vessel contains several control systems. Power management system, cargo control system, automatic sailing system, drilling system, propulsion control and dynamic positioning systems are all control systems used in advanced marine vessels (Sørensen, 2005). The dynamic positioning system consists of various sensors, hardware and software. Measurements to the DP system are provided by position reference systems (e.g. GPS) and sensors (e.g. Compass, wind gauge). In a control algorithm these measurements are used to calculate the required thrust force to stay on the desired reference position. The control signal is processed in a thrust allocation algorithm which finally commands the thruster action.

The regulator can again be divided into controller, observer and in the case of supervisory control, a supervisor. The main focus of this thesis is on the software and development of regulator algorithms suitable for use in arctic areas. The functionality and design of these components are accounted for in the following.

4.1 Observer design

The observer is used to provide the controller with reliable estimation of the process states (vessel position and velocity). The observer produces estimates of states that are difficult to measure, and can also be used to remove measurement noise by filtering the signal. In DP systems, the observer is usually also used to remove the wave frequency of the position measurements since the wave forces that cause this movement have a zero time average and will not give any resulting drift-off from the desired position. Removing the wave frequency motions from the feedback loop reduces wear and tear on the propulsion system.

To provide good estimates the observer should copy the vessel dynamics using only the measurable states and the command signal as input.

4.1.1 Open water observer

A nonlinear passive observer is selected for the open water case. Fossen (2002, p.203) gives the observer equations:

$$\dot{\hat{\boldsymbol{\xi}}} = \mathbf{A}_{\omega}\hat{\boldsymbol{\xi}} + \mathbf{K}_1\tilde{\mathbf{y}} \tag{4.1}$$

$$\dot{\hat{\boldsymbol{\eta}}} = \mathbf{R}(y_3)\hat{\boldsymbol{\nu}} + \mathbf{K}_2\tilde{\mathbf{y}} \tag{4.2}$$

$$\dot{\hat{\mathbf{b}}} = -\mathbf{T}^{-1}\hat{\mathbf{b}} + \mathbf{K}_3\tilde{\mathbf{y}} \tag{4.3}$$

$$\mathbf{M}\dot{\hat{\boldsymbol{\nu}}} = -\mathbf{D}\hat{\boldsymbol{\nu}} + \mathbf{R}^T(y_3)\hat{\mathbf{b}} + \boldsymbol{\tau} + \mathbf{R}^T(y_3)\mathbf{K}_4\tilde{\mathbf{y}} \tag{4.4}$$

$$\hat{\mathbf{y}} = \hat{\boldsymbol{\eta}} + \mathbf{C}_{\omega}\hat{\boldsymbol{\xi}} \tag{4.5}$$

where $\hat{\boldsymbol{\xi}} \in \mathbb{R}^{6\times 6}$ is the estimate of the state vector for modeling of linear wave response, $\hat{\eta} = \begin{bmatrix} \hat{\eta} & \hat{e} & \hat{\psi} \end{bmatrix}^T$ is the estimate of position and heading, $\hat{\mathbf{b}}$ is bias estimation vector, $\hat{\boldsymbol{\nu}}$ is velocity estimation vector, $\tilde{\mathbf{y}} = \mathbf{y} - \hat{\mathbf{y}}$ is the estimation error, $\mathbf{R}$ is the rotation matrix defined in (2.16), $\mathbf{A}_{\omega} \in \mathbb{R}^{6\times 6}$ is the wave frequency system matrix, $\mathbf{M}$ is the vessel mass matrix, $\mathbf{D}$ is the vessel damping matrix and $\mathbf{K}_1 \in \mathbb{R}^{6\times 3}$ and $\mathbf{K}_{2,3,4} \in \mathbb{R}^{3\times 3}$ are observer gain matrices.

4.1.2 Ice observers

The observer presented in 4.1.1 may perform well under open water conditions, but when there are ice forces present, the estimates may not be satisfactory. An observer which takes the ice forces into account would probably give a more accurate state estimation. In the same way as equation (4.3) accounts for slowly-varying environmental disturbances, we can modify the open water observer to get an observer with ice force estimation. As there will be very little waves when the ship is moving into the ice regime, we do not want to use wave filtering. Modifying the open water observer with these points in mind, we end up with the following equations for the ice observers

$$\dot{\hat{\boldsymbol{\eta}}}_T = \mathbf{R}(y_3)\hat{\boldsymbol{\nu}} + \mathbf{K}_2\tilde{\mathbf{y}} \tag{4.6}$$

$$\dot{\hat{\mathbf{b}}} = -\mathbf{T}^{-1}\hat{\mathbf{b}} + \mathbf{K}_3\tilde{\mathbf{y}} \tag{4.7}$$

$$\dot{\hat{\boldsymbol{\tau}}}_{ice} = -\mathbf{T}_{ice}^{-1}\hat{\boldsymbol{\tau}}_{ice} + \mathbf{K}_{51}\tilde{\mathbf{y}} \tag{4.8}$$

$$\mathbf{M}\dot{\hat{\boldsymbol{\nu}}} = -\mathbf{D}\hat{\boldsymbol{\nu}} + \mathbf{R}^T(y_3)(\hat{\mathbf{b}} + \hat{\boldsymbol{\tau}}_{ice}) + \boldsymbol{\tau} + \mathbf{R}^T(y_3)\mathbf{K}_4\tilde{\mathbf{y}} \tag{4.9}$$

$$\hat{\mathbf{y}} = \hat{\boldsymbol{\eta}}_T \tag{4.10}$$

where $\mathbf{K}_{51} \in \mathbb{R}^{3\times 3}$ is an ice load gain matrix and $\hat{\boldsymbol{\eta}}_T$ is the total estimated motion. If the ice forces can be measured (by use of strain gauges or inertial measurements), equation (4.8) can be replaced with

$$\dot{\hat{\boldsymbol{\tau}}}_{ice} = -\mathbf{T}_{ice}^{-1}\hat{\boldsymbol{\tau}}_{ice} + \mathbf{K}_{51}(\mathbf{R}(\mathbf{y}_3)\boldsymbol{\tau}_{ice} - \hat{\boldsymbol{\tau}}_{ice}) \tag{4.11}$$

where $\boldsymbol{\tau}_{ice}$ is the vector of ice load measurements.

The ice observer can be used for estimation in both broken ice and level ice conditions, but the observer gain matrices should be tuned differently for the two operating conditions. The time constant $\mathbf{T}_{ice}$ is also a parameter that can affect the performance of the ice observers, and should be tuned to its use. The level ice time constant should be less than the open water bias time constant and the time constant for broken ice observer should be even lower. This is to ensure that the ice forces are captured by the estimator as early as possible.

The level ice loads are larger than the broken ice loads, so the ice load gain matrix for level ice should be tuned to a high value. Details on the time constants and gain matrices for the observers can be found in the appendix.

4.2 Control law design

4.2.1 PID controller

Control laws for dynamic positioning systems are usually of the PD type with integral action (Sørensen, 2005). A PID controller with estimated LF motion as input is chosen for both open water and ice conditions. If there are measurements of the ice forces available, there should be implemented a feedforward control term of the ice forces. The control signal will then consist of the control forces calculated by the PID controller plus the feedforward term:

$$\boldsymbol{\tau} = -\mathbf{K}_p\tilde{\boldsymbol{\eta}} - \mathbf{K}_d\tilde{\boldsymbol{\nu}} - \mathbf{K}_i\int_0^t \tilde{\boldsymbol{\eta}}(\tau)d\tau + \boldsymbol{\tau}_{FF} \tag{4.12}$$

In the simulations performed in chapter 5 it is assumed that the ice force measurements are not available and ice load feedforward is therefore not included in the controllers.

The ice controllers should be tuned with higher gains than the open water controller to quickly eliminate the impact of the ice loads. The change in integral gain is considered to be of particular importance, as the ice loads contains a significant mean loading in one direction which would have to be counteracted by the integral action of the controller. With the more aggressive controller in addition to the improved position and velocity estimates from the ice observers, we should expect an improvement on the position keeping capabilities.

The offline controllers will develop as if they were connected to the plant, and the integrator in the open water controller will continue to build up during the time in the ice regime. If the vessel exits the ice when the integrator in the open water controller has built up a large force, switching to this controller will cause an overshoot of the desired position due to the sudden decrease in environmental loads. The integrator may therefore need to be reset to zero before the switching is performed. This is implemented in the open water controller only, as the switching to the ice controllers is dependent on the increased control force given by the integrator build up.

Details on the gain matrices used in the simulations can be found in Appendix B.

4.2.2 Weather-optimal positioning control

To reduce the ice forces on the ship when performing station keeping in ice, it is very important to keep the bow up against the drifting ice. When the ice hits the vessel bow, it will act on a much smaller area than if it hits on one of the sides of the ship and hence give less loading on the vessel. The bow is usually the only part of the ship that is able to break ice as the vessel sides have a much steeper stem angle. The bow will also direct the ice floes to the sides and past the vessel.

It is not feasible to measure the varying ice drift direction directly. To make sure that the vessel bow is directed towards the drifting ice one could therefore consider to use the weather optimal positioning control scheme (WOPC) proposed by Fossen & Strand (2000) modified for use in an ice regime.

The WOPC control scheme is motivated by a pendulum in a gravity field where the pendulum eventually will stabilize at the bottom equilibrium position where it has the least potential energy (see Figure 20). If the vessel is commanded to point towards a fixed point (x_0, y_0) (corresponding to the pendulum pivot point) and to keep a given distance to this point (the length of the pendulum rod), the environmental forces will eventually push the vessel along the circle arc and rotate it such that the vessel bow is directed against the resulting environmental loads.

This is obtained by specifying the control objective in polar coordinates according to $\rho_d = \text{constant}$, $\dot{\gamma}_d = 0$ and $\psi_d = \pi + \gamma$, where the first requirement keeps the vessel on a circle with constant radius, the second requirement keeps the tangential speed low, and the third requirement ensures that the vessel bow points towards the circle center.

The vessel position in polar coordinates is given by

$$\begin{aligned} \rho &= \sqrt{(x - x_0)^2 + (y - y_0)^2} \\ \gamma &= \text{atan2}((y - y_0),(x - x_0)) \\ \psi &= \psi \end{aligned} \tag{4.13}$$

where $p_0 = \begin{bmatrix} x_0 & y_0 \end{bmatrix}^T$ is the center of a circle.

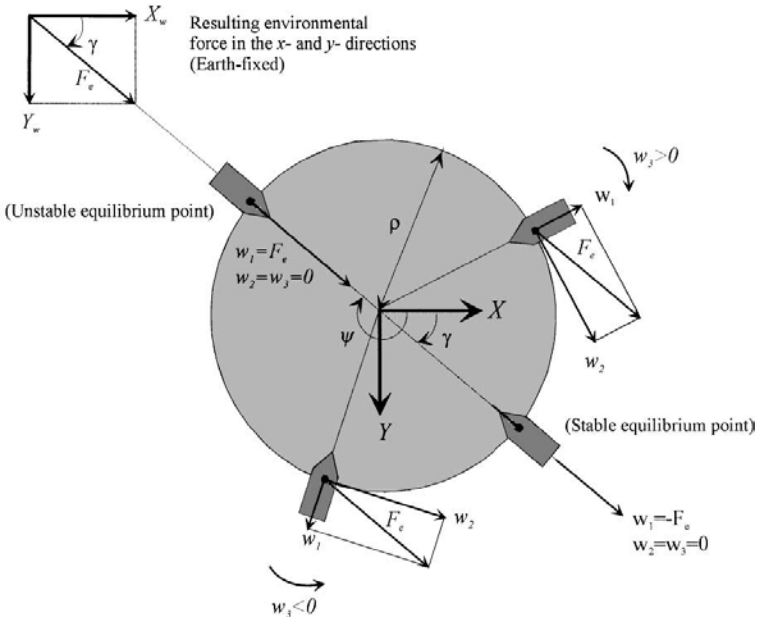

Figure 20 Weather optimal positioning motivated by a pendulum (Fossen & Strand, 2000)

If, in addition to the requirements above, the circle center is moved such that the ship moves along a virtual circle arc, but maintains a constant earth-fixed position, the vessel will be able to perform station-keeping with weather-optimal heading. The ship will then keep its position, but rotate a yaw angle until it reaches the optimal heading. This is referred to as translational circle center control.

The WOPC equations derived by Fossen & Strand (2000) can be found in Appendix A.

4.3 Supervisor

The supervisor modified for use with the concept of spectral analysis of the vessel motion is shown in Figure 21. The supervisor's task is to buffer the pitch motion measurements, perform an FFT analysis on the buffered signal and compare the resulting frequency spectrum with the model frequency spectra introduced in section 3.2-3.4.

The frequency spectra for waves and ice conditions have very different amplitudes. If we would attempt to compare the model frequency spectra directly, we would experience problems with scaling of the results. As the open water frequency spectrum contains mostly large amplitudes, the error between the spectrum calculated online based on measurements and the model spectrum would be large in absolute value even though the vessel was actually in an open water regime. Both the response spectrum calculated online and the spectra of the process models are therefore normalized to a unit length before they are compared against each other. The norm of the resulting vectors of spectrum amplitude differences are then fed to the monitoring signal generator.

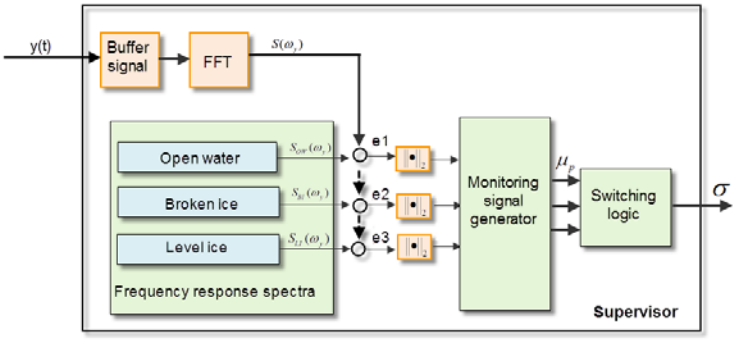

Figure 21 Supervisor components with FFT

4.3.1 FFT and buffer

The FFT analysis performs a Discrete Fourier transform which converts the pitch motion from time domain to the frequency domain. The transformation for vectors of length N is given by

$$X(k) = \sum_{j=1}^{N} x(j)\omega_N^{(j-1)(k-1)}$$
$$\omega_N = e^{(-2\pi i)/N} \tag{4.14}$$

To make sure that the most important frequency components are captured by the FFT analysis, the signal needs to be buffered for some time. The longer the signal is buffered (larger N), the better the

estimate of the frequency spectrum will be. The FFT analysis may be performed each time the buffer reaches a predefined number of samples. This will, however, give a very slow update for the online calculation of response spectrum. The buffer block should therefore overlap each output by most of the buffer length. This way, the update rate of the frequency spectrum will be faster, while information from all of the buffer length is used and the old information in the time signal is gradually replaced with new signals.

One drawback with using frequency spectra as model identification in the supervisory control system, is that the buffered signal will always contain historic signals, i.e. even though the vessel response may have changed, the buffered signal may still be dominated by motions from the "old" condition. This is the case for the transition between open water with wave movement to level ice without waves. The pitch motion in waves has much higher amplitude than the motion inside the level ice regime. The buffered signal will therefore be dominated by the wave motion for some time into the level ice regime. It is therefore important to select the buffer length and overlap with care.

4.3.2 Switching logic

The dwell-time switching logic is not adequate for non-linear systems due to the problem of finite escape time (Hespanha, 2002). The vessel dynamics considered here is indeed non-linear, and we should therefore use the scale-independent hysteresis switching logic which does not have the same problem with nonlinearities.

5 Simulation study

When designing and analyzing DP control systems it can be a very efficient tool to simulate the dynamically positioned vessel's response to external forces on a computer. In this thesis we will use a module-based simulator called Marine Cybernetics Simulator (MCSim) in Matlab/Simulink developed by students and researchers at NTNU to test the proposed controllers and ice force modules.

In order to evaluate the performance of the supervisory control presented in chapter 4, several simulation scenarios are performed. The main focus is to evaluate the switching logic when the ice conditions changes between open water and level ice. Performance with regular open water controller is compared to supervisory control performance in a number of tests.

5.1 Input data

5.1.1 Vessel model

The vessel model used in the simulations is the MC supply as given in the MCSim simulator with some modifications in the bow geometry for icebreaking capabilities. The vessel dimensions were given in section 3.2.1 but are included here in Table 5 as well for reference.

MC Supply	
Length	80 [m]
Breadth	17.4 [m]
Draft	5.6 [m]
Displacement	6000 [m^3]
Bow stem angle	24°
Side stem angle	90°

Table 5 MC Supply dimensions

The thruster dynamics of the vessel actuators are approximated by a simplified 1st order model which basically smoothens the thruster forces and introduces some delay before the forces are applied to the vessel. The dynamics are given by

$$\dot{\tau} = A_{thr}^{-1}(\tau_c - \tau) \tag{5.1}$$

Where τ is the output of the thruster dynamics, τ_c is the command signal from the controller and A_{thr} [4] is a diagonal matrix of time constants.

5.1.2 Simulation setup

The tests are performed with open water environmental loads as specified in Table 6. These environmental loads will be used throughout the simulations in ice also, except that the wave motion is disregarded during the time when the vessel in an ice regime. Near the ice edge and in the ice regime,

[4] $A_{thr} = diag\begin{bmatrix}1 & 1 & 1\end{bmatrix}$ in the simulations

the wave height will be limited. Significant wave height is therefore chosen as 0.5 m with no waves once the bow hits the level ice.

Environmental forces	
Significant wave height	0.5 [m]
Mean wave direction	180°
Mean wind velocity	8.0 [m/s]
Mean wind direction	180°
Current velocity	0.3 [m/s]
Current direction	180°

Table 6 Open water test environmental forces

The ice condition used in the simulations is level ice with parameters as specified in Table 7. An ice thickness of 0.5 meters and drift velocity of 3 [m/s] is considered probable conditions in the relevant arctic operating areas.

Ice conditions	
Ice regime	Level ice
Compressive strength	$5 \cdot 10^6$ [Pa]
Flexural strength	$6 \cdot 10^5$ [Pa]
Ice thickness	0.5 [m]
Young's modulus	$5.4 \cdot 10^9$ [Pa]
Ice drift velocity	0.3 [m/s]

Table 7 Level ice condition

The case considered in these simulations is the vessel performing station keeping in open water being hit by a drifting level ice sheet. Four case studies are performed.

	Case 1	Case 2	Case 3	Case 4
Ice	300s open water 300s level ice 400s open water	300s open water 300s level ice 400s open water	500s open water 500s level ice	500s open water 500s level ice
Ship heading	0°	0°	22.5°	22.5°
Controller bank	Open water	Open water PID Level ice PID	Open water PID Level ice PID	Open water PID Level ice WOPC

Table 8 Description of simulation cases

Case 1 & 2

The simulations in case 1 and 2 are performed for 1000 seconds, where the first 300 seconds are open water condition with waves, then 300 seconds of level ice and finally 400 seconds of open water and waves again. From 600-700 seconds, the bow has entered the open water area, and only friction forces on the ship side are present. This is approximated by the surge ice load at 600 seconds is gradually reduced to zero during the next 100 seconds. Even though the ice sheet will not have drifted the entire vessel length (80 m) those 100 seconds, the friction forces are small when most of the vessel has exited the ice, and they are therefore disregarded these last seconds. Figure 22 shows a sketch of the time history of the ice drifting past the vessel. The vessel is supposed to maintain its position when the ice

hits, and also keep the position through the ice and when it exits the ice regime and enters open water again.

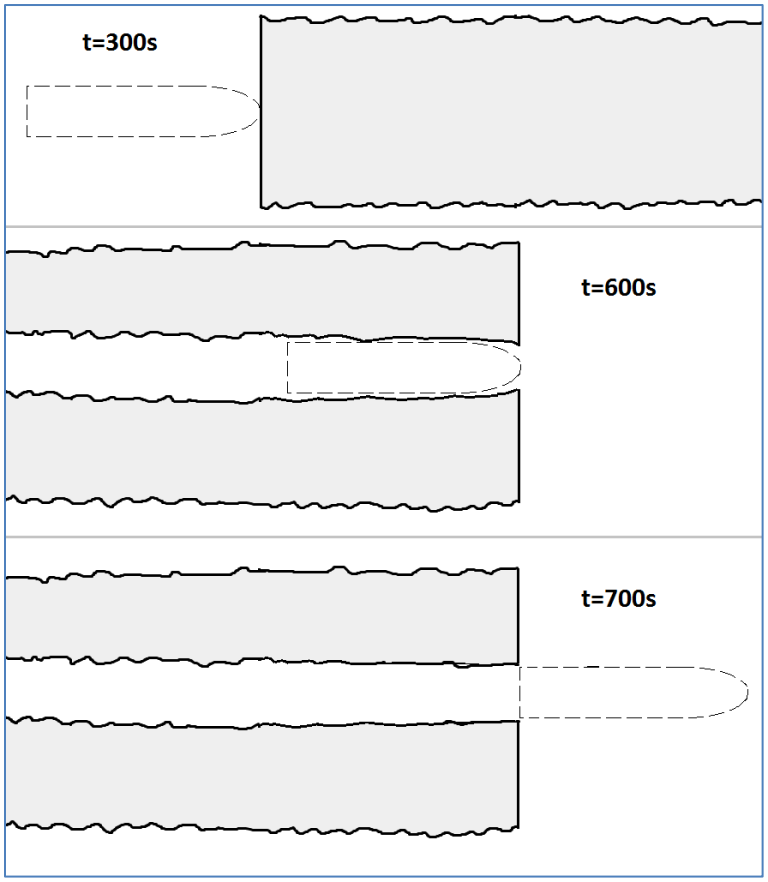

Figure 22 Ice drifting events

Case 3 & 4

The simulations in case 3 and 4 consists of 500 seconds of open water condition before the vessel is hit by a drifting level ice sheet which has a relative angle of 22.5 degrees to the vessel. The environmental and ice conditions are the same as in the first case simulation, but the vessel is commanded to keep a heading of 22.5 degrees. The open water observer bias and controller integrator is initiated with initial conditions close to the total environmental loads to reduce transients towards the reference position. Two controller settings are considered: Case 3 use the same supervisory control scheme as in section case 2 with switching between open water controller and the level ice PID controller. Case 4 use the supervisory control scheme with PID controller for the open water regime and the WOPC controller presented in section 4.2.2 for the ice regime.

Figure 23 Ice drift angle sketch

5.2 Results

5.2.1 Case 1: Traditional control comparison

The following plots shows results from simulation with traditional open water control. That is, the open water observer without ice estimation and open water PID controller gains was used throughout the simulations. The reference position was kept as $\eta_{ref} = \begin{bmatrix} 0 & 0 & 0 \end{bmatrix}^T$ throughout the simulation.

Figure 24 shows that the ice loads starts when vessel hits the ice edge after 300 seconds, and increases until the most of the ship length is in the level ice at 400 seconds. The level ice load shows the ice breaking as high frequency peaks in the load curve. At 600 seconds the ship bow leaves the ice. Only friction force against the ship sides are left, and this decreases towards zero during the next 100 seconds.

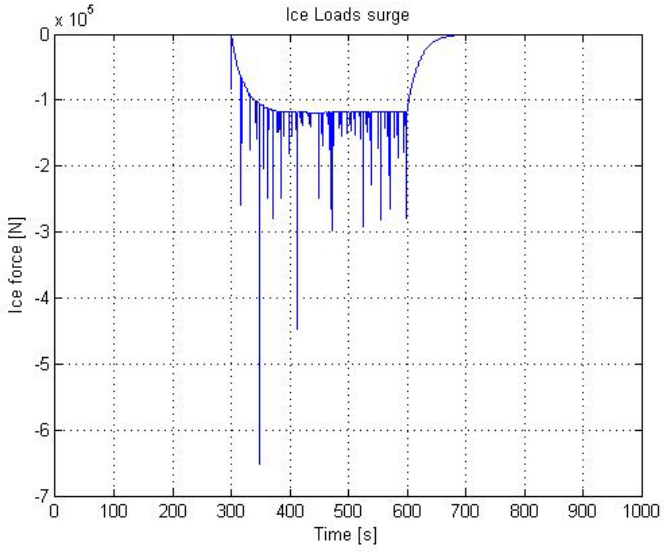

Figure 24 Level ice test surge ice loads

The position measurements of the simulation is shown in Figure 25 where we see that the vessel is pushed back by the ice sheet from 300 to 400 seconds, and reaches an error in north direction of 4 meters. Although the vessel hits the ice head on, there are still some loads causing sway and yaw displacements.

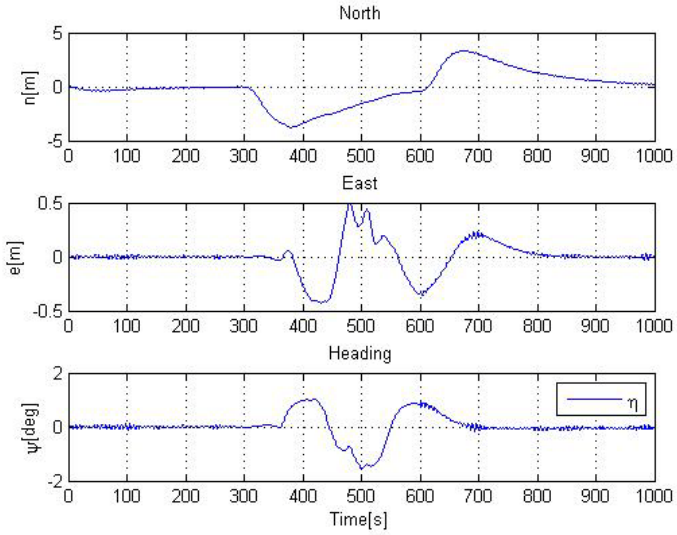

Figure 25 Open water - level ice using traditional control

The open water DP system manages to recover the reference position after 600 [s], but when the vessel exits the ice at this point, the excessive thruster forces cause the vessel to overshoot the reference position and reach an error of 4 [m] in the positive north direction as well. The total commanded control force is shown in Figure 26. We see that there is a significant commanded force in surge direction when the vessel leaves the ice at 600 [s].

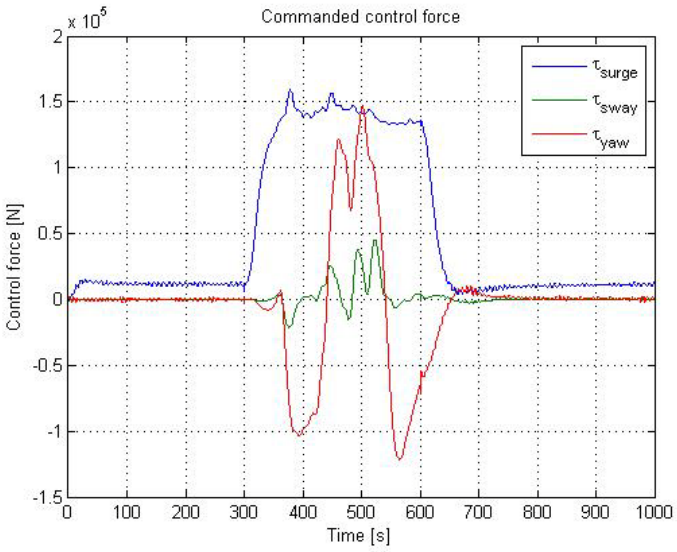

Figure 26 Open water controller commanded force

Looking at the proportional, integral and derivative terms in the PID controller action, shown in Figure 27, we see that the overshoot is due to the build-up of the integrator action which takes some time to discharge.

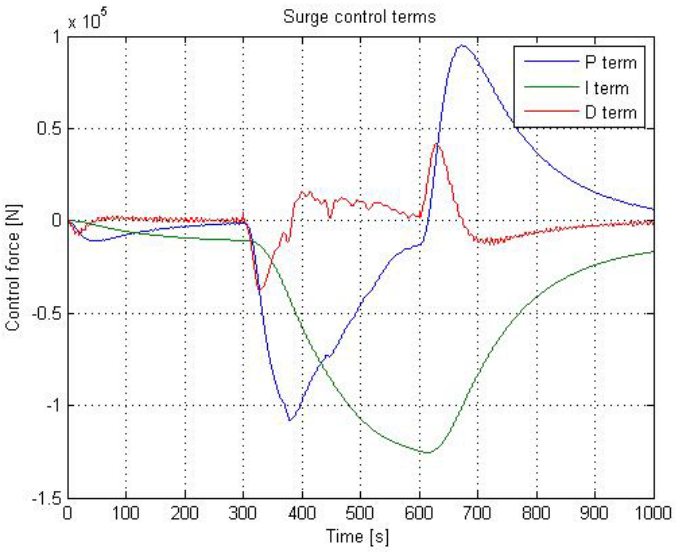

Figure 27 Open water controller PID terms

5.2.2 Case 2: Supervisory switching

The transition from open water to level ice is an abrupt change from no ice loads to forces up to several hundred kN in only a few seconds. The ability to handle this kind of sudden process changes is one of the key attractive properties of the supervisory control strategy.

Figure 28 shows the monitoring signals and the switching signal where we see that the open water monitoring signal is small from 0s-315s and from 605s-1000s. The signals clearly shows that one process model is a better fit than the other in both operating regimes (open water and level ice).

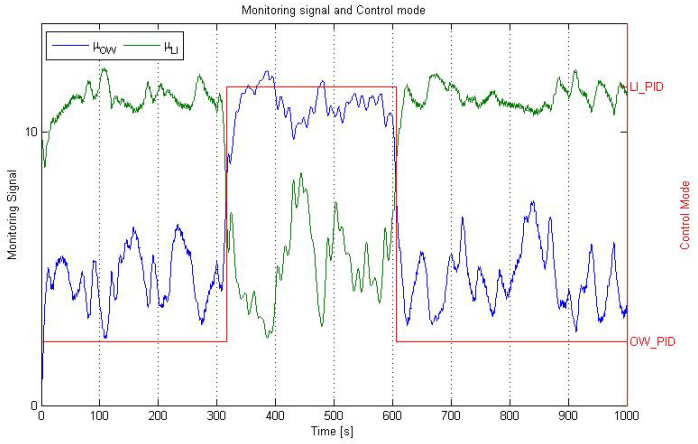

Figure 28 OW-LI-OW Monitoring signals and switching signal

The supervisor switches to the level ice PID controller (LI_PID) 16 seconds after impact with the level ice, and back to open water controller (OW_PID) 6 seconds after the bow leaves the ice.

The reason that the switching back to open water is faster is that the wave motion dominate the frequency spectrum even if the buffered position signal contains some period of ice load induced motions.

In Figure 29 we see that the maximal deviation from the desired position is reduced to 1.5 meters using the supervisory-switched control. When the vessel leaves the ice at 600 [s], the supervisor switches back to the open water controller. In contrast to the simulation using open water controller, the integrator action is reset at this point, and the vessel is pushed back approximately one meter instead of having an overshoot of the reference position.

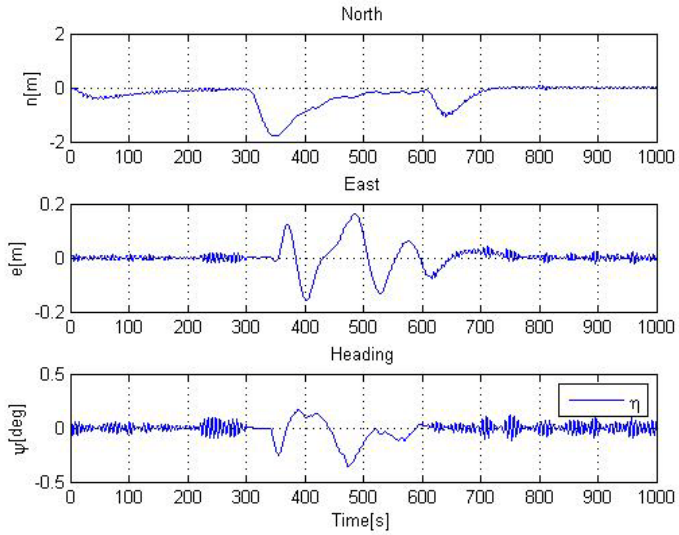

Figure 29 OW-LI-OW Position time series

The increased performance of the DP system compared to the regular open water controller is much due to the increased gains in the level ice PID controller, but also because of increased accuracy of the observers. Especially the velocity estimation is affected by the ice conditions. In Figure 30 the difference between estimated velocity in surge direction and the actual low-frequency velocity is shown. The level ice observer without wave filtering has large variations in the open water condition, as expected. When the vessel hits the level ice after 300 seconds, both observers shows a peak in the surge velocity estimate errors due to the sudden ice load. It can be seen that from this point, the level ice observer provides the best velocity estimates, until the wave motion is initiated again when the vessel leaves the ice regime at 600 second.

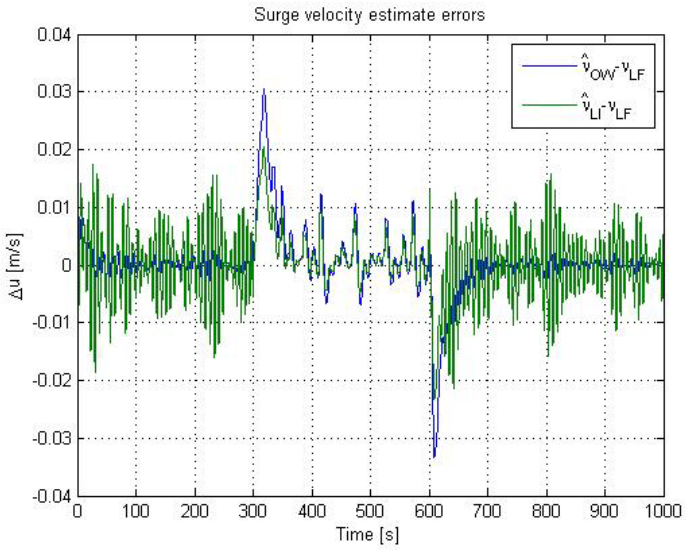

Figure 30 Surge velocity estimate comparison

If we look at the commanded control forces shown in Figure 31, we see that the bumpless transfer scheme ensures a more or less smooth transition from the open water to level ice controller at t=316 [s]. When the supervisor switches back to the open water controller, however, there is a large jump in control command at t=606 [s]. This is because of the resetting of open water integrator action at this point. This should ideally have been avoided by the bumpless transfer (BT) action, but when the integrator is emptied as suddenly as it is done here, the BT states does not keep up, and the result is a jump in the command signal. Since the system matrix of the BT block is not Hurwitz, this also means that the state stabilizes at a non-zero value and commands a wrong reference position to the controller. This is solved in an ad hoc manner by also resetting the states of the BT block when the controller integrator is reset. Hence, the reference signal to the controller will be correct, but at the cost of a sudden step in the control signal.

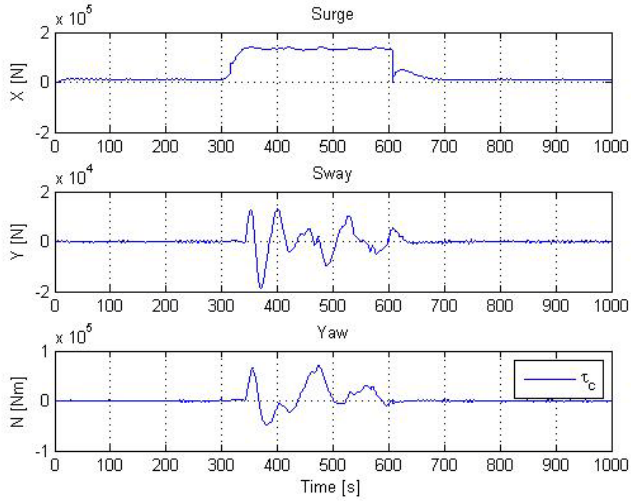

Figure 31 Control commands

5.3 Variation of parameters

There are several parameters which have direct influence on the performance of the supervisory control system. The most important are the hysteresis constant h, the forgetting factors λ and the buffer length of the pitch signal for the FFT. These parameters control the desire to switch to the smallest estimation error to satisfy the small error property against the risk of too fast switching which may violate the non-destabilization property. A small hysteresis constant, large forgetting factors and a short buffering time may give fast adaptation to changing conditions but could cause switching back and forth between controllers only due to some noise or other random processes influencing the process. A large hysteresis constant, small forgetting factors and long buffering time, on the other hand, will give reliable estimation of the current operating process, but may use too long time before a new controller is selected when the conditions are changing.

5.3.1 Buffer time

The length of the buffered pitch motion signal is of vital importance to the supervisory system ability to detect the changing conditions. Long buffer time gives good resolution on the frequency spectrum, i.e. the dominant frequencies are recognized more accurately, but the long buffer time will also lead to "old" measurement influencing the frequency spectrum for a longer time. A short buffer time ensures that the measurements used in the FFT analysis are of recent events and should therefore lead to a shorter detection time. The short buffer time may, however, lead to wrong conclusions being drawn from the FFT analysis because of the reduced resolution of the frequency spectrum, and consequently order the switching logic to select the "wrong" controller.

Figure 32 shows the results from the parameter sensitivity analysis where the buffer length was varied to assess the detection time. Several simulations were performed under the same environmental conditions and controller settings as earlier with varying buffer time settings. The sample time was 0.01[s] and the buffer length was set to

$$N_{FFT} = 2^i \quad i = 8,9,...,14 \tag{5.2}$$

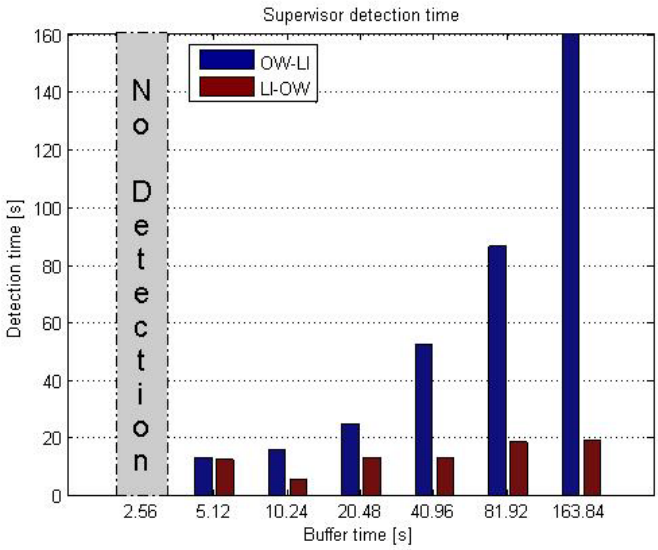

Figure 32 Detection time vs. buffer time

The figure shows the detection time from open water to level ice (OW-LI) and vice versa (LI-OW). The detection time from ice to open water is generally much shorter that the detection of ice because the buffered signal will be dominated by the wave motion. The buffer length dependency of detection time is clearly seen from the increasing bars. When the buffer length was set to 256 samples, the supervisor was not able to detect the ice and switch controller. This is due to the low resolution of the frequency spectrum when the FFT analysis is based on only 256 samples. The resolution of the FFT analysis can be calculated as

$$\Delta\omega = \frac{2\pi}{N_{FFT}T_s} = \frac{2\pi}{256 \cdot 0.01} = 2.45[rad\ /\ s] \tag{5.3}$$

where T_s is the sample time and N_{FFT} is the number of samples in the FFT, denoted as buffer length. The FFT analysis will divide the frequencies into "bins" with width $\Delta\omega$, where each bin contains the energy from a frequency range. The bin of the lowest frequencies is half the width of the other bins (the FFT considers both positive and negative frequencies, and hence the one bin centered around zero frequency has half the width containing positive frequencies). To be able to detect the difference between the two model spectra of level ice and open water, the energy from the peak frequencies of the frequency spectra should end up in different bins. The FFT resolution should therefore be at least the difference between the dominating wave frequency and the peak at zero frequency in the level ice model spectrum. For the case simulated here, this corresponds to

$$\Delta\omega < \omega_{peak} - 0 \Rightarrow N_{FFT} > \frac{2\pi}{(\omega_{peak} - 0)T_s} = 676 \tag{5.4}$$

To be able to detect the peak at the normal frequency, the resolution should be even smaller, and the buffer length should be

$$N_{FFT} > \frac{2\pi}{(\omega_{peak} - \omega_{0,5})T_s} = 1461 \tag{5.5}$$

For the case of separation of only two different regimes, as considered in this simulation study, a buffer length of 1024 gives a resolution which is able to separate the two frequency spectra due to the peak at zero frequency in the level ice model spectrum, which is also seen from the simulations. A smaller buffer length is not recommended unless the sampling rate is increased.

5.3.2 Forgetting factors

The monitoring signal given by (2.6) includes the choice of forgetting factors, λ, which influence the dynamics of the monitoring signal. Increasing the forgetting factor corresponding to either process model, will give faster forgetting of old error measurements while decreasing the forgetting factor will increase the memory of the monitoring signal, i.e. the historic measurements will have more influence on the signal.

To reduce the detection time from open water to level ice one might want to increase the forgetting factor of the level ice monitoring signal. A parameter study on the choice of forgetting factors is done by performing two more simulations with increasing level ice forgetting factor. The open water forgetting factor is kept constant in both simulations. The environmental conditions and controller settings are also the same as in case 2.

Figure 33 shows the results from the case when $\lambda = \begin{bmatrix} \lambda_{OW} & \lambda_{LI} \end{bmatrix} = \begin{bmatrix} 0.10 & 0.15 \end{bmatrix}$ where it can be seen that the detection time from open water to level ice is reduced from 16 seconds to 12 seconds. This also gives a better counteraction of the ice loads and some reduction of error in north direction. The monitoring signals still gives a good decision basis for the switching logic.

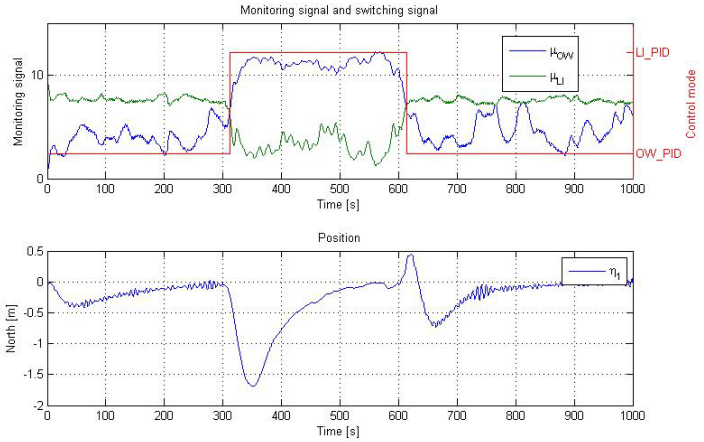

Figure 33 Results from λ_{LI}=0.15

Figure 34 shown the result when $\lambda = \begin{bmatrix} \lambda_{OW} & \lambda_{LI} \end{bmatrix} = \begin{bmatrix} 0.10 & 0.20 \end{bmatrix}$ where we see that the level ice monitoring signal is stabilized at a too low level compared to the open water signal. Since the generated monitoring signal does not provide the switching logic a good basis for deciding the controller switching,

the supervisor switches back and forth between the open water controller an level ice controller. From the north position shown in the bottom of Figure 34, we see the influence of changing controller as oscillations around zero in the open water regime. This is due to the discharging of the open water controller each time the supervisor switches from the level ice controller to the open water controller.

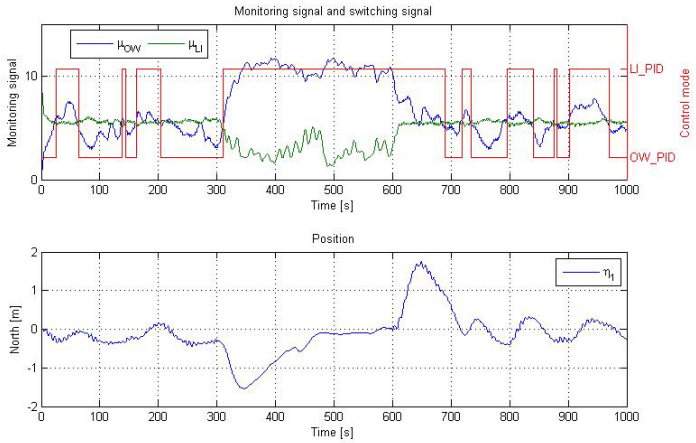

Figure 34 Results from λ_{LI}=0.20

These two simulations show that it is possible to reduce the detection time by altering the generation of the monitoring signal, but too much increase of the forgetting factor may lead to excessive switching. This is in accordance with the non-destabilization property for the scale-independent hysteresis switching logic (2.8) where it is stated that an increase in forgetting factor may lead to a higher number of discontinuities in the switching signal.

5.3.3 Hysteresis constant

The hysteresis constant is important to select such that switching is not performed unless the monitoring signal shows clearly which process model is the most likely one. For the case of weakly detectable process models, the hysteresis constant may have to be set to a relatively high value to prevent switching back to the original controller shortly after the first switch (as was the case in the project thesis by Skogvold (2009)). For the case of detection based on FFT analysis, the monitoring signals seem to show clear trends in which process model is closest to the ongoing process, and the hysteresis constant can be selected quite low. In the simulations performed above, the hysteresis constant was set to $h = 0.1$. This means that the supervisor will switch to a new controller once the monitoring signal of the current process model is 10 percent larger than the monitoring signal of the best fit model. The hysteresis constant should be selected high enough to reduce excessive switching and prevent chattering but low enough to get the desired switching.

5.4 Ice drift angle

A case with ice drifting from an angle is performed to show the limitations of the level ice PID controller. A simulation where the level ice PID controller is replaced with a controller based on the weather-optimal positioning control principle is performed to show one of the nice properties of supervisory control, namely the ability to implement off-the-shelf controllers in the system.

5.4.1 Case 3: Supervisory control using PID controllers

The same supervisory control system as in case 2, with a small increase in level ice forgetting factor[5] to reduce detection time (as shown in section 5.3.2), is used to keep the position (and heading). Figure 35 shows the monitoring signal and the switching between open water PID controller (OW_PID) and level ice PID controller (LI_PID) where it is noted that the detection time is around 12 seconds, as was also the case in the head on encounter with increased forgetting factor.

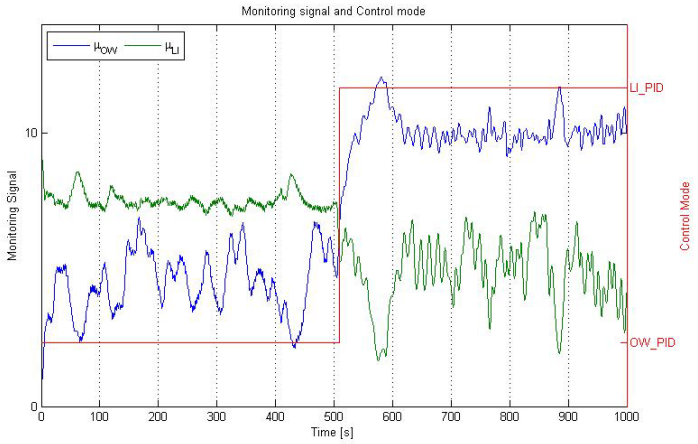

Figure 35 Monitoring signal and switching signal

Although the supervisor switches to the level ice PID controller relatively shortly after the ice sheet hits the vessel, Figure 36 shows that the new controller is not able to keep the position. The controller manages to keep the position for some time after the initial ice hit because bow hits the ice first, and the vessel breaks the ice. When the ice reach the vessel sides, however, the position is lost. After 200 seconds in the level ice regime, the ice loads are too intense, and the vessel heading reaches more than 90 degrees, i.e. the ice is pushing against the broadside of the vessel. This in turn leads to extreme position offsets in surge and sway. Hence, the vessel experience a complete loss of position.

[5] $\lambda = \begin{bmatrix} \lambda_{OW} & \lambda_{LI} \end{bmatrix} = \begin{bmatrix} 0.10 & 0.15 \end{bmatrix}$

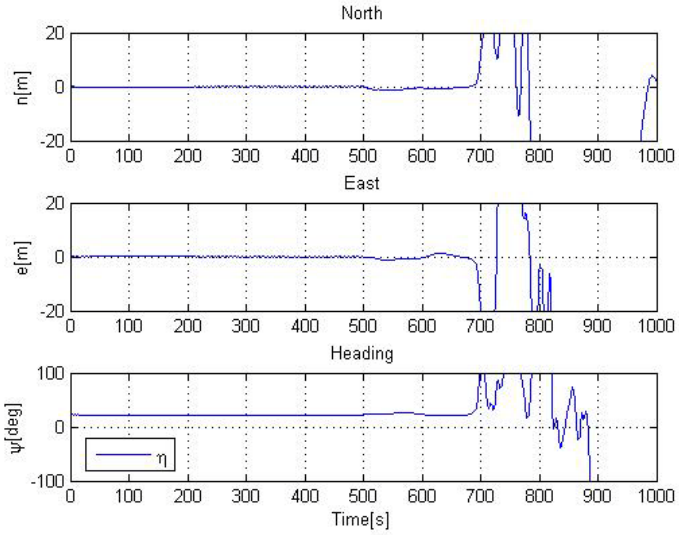

Figure 36 Position time series

5.4.2 Case 4: Supervisory control with WOPC

The level ice PID controller is replaced with the weather-optimal positioning control scheme presented in section 4.2.2 using the level ice observer for position and velocity estimates. The supervisory control system is supposed to detect the ice and switch to the WOPC controller which in turn shall make sure that the vessel bow eventually is directed towards the drifting ice, where the ice loads will have the least impact on the vessel. This simulation is performed without the bumpless transfer implemented.

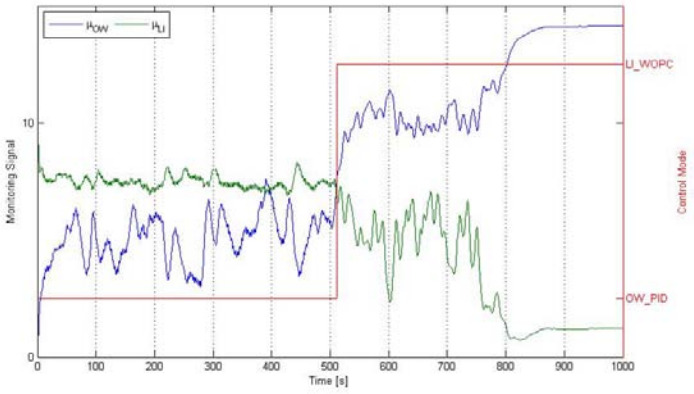

Figure 37 Monitoring signal and switching signal

Figure 37 shows that the supervisor selects the level ice WOPC controller (LI_WOPC) shortly after the ice hits and keeps the controller throughout the rest of the simulation. It is noticed that the monitoring signal changes shape the last 200 seconds of the simulation. This is due to a problem with the calculation of ice breaking loads when the ice encounters the bow from an angle. The vessel bow has a relatively low stem angle to ensure ice breaking abilities, but the vessel sides are 90 degrees and only crushing loads are present here. When there is no ice breaking along the vessel side, this may lead to errors in the update of ice geometry here, and causing the vessel to pass over the ice edge without any

subsequent breaking loads being calculated. Figure 38 shows the total ice loads in surge, where we see that the breaking loads are missing from the last 200 seconds of the simulation.

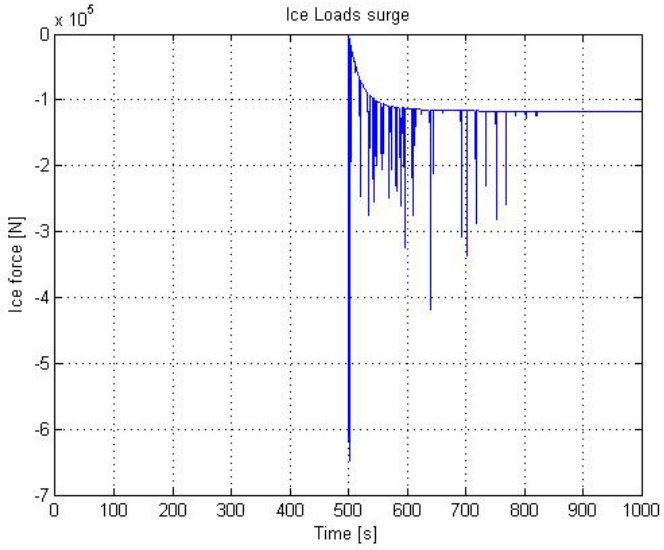

Figure 38 Missing ice breaking loads

The ice load calculations will, however, include the magnitude and direction of the ice resistance and the concept of weather-optimal positioning is effectively demonstrated.

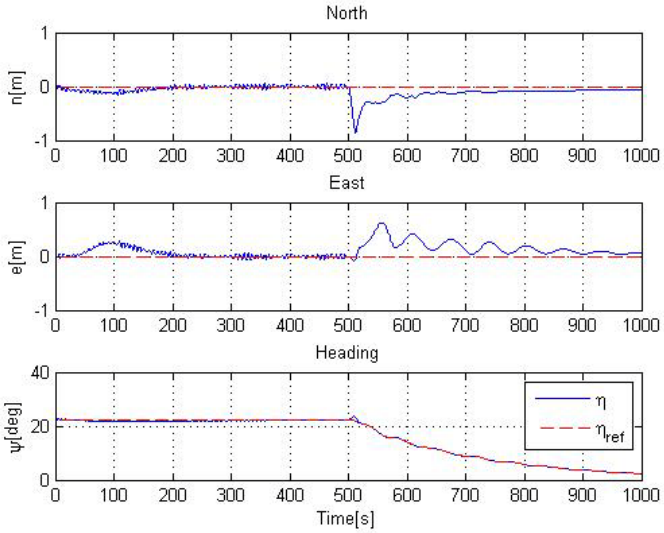

Figure 39 Position and reference

Figure 39 shows the reference and measured position time series. When the WOPC controller is selected shortly after 500 seconds, the heading reference is 22.5 degrees, but as the vessel is pushed by the ice along the imaginary circle arc, the reference heading is gradually changed towards the resulting environmental load direction at zero degrees. This is achieved without any measurements of the ice

loads. The north and east position measurements shows very small deviations from the reference position, and the vessel keeps the position throughout the simulation.

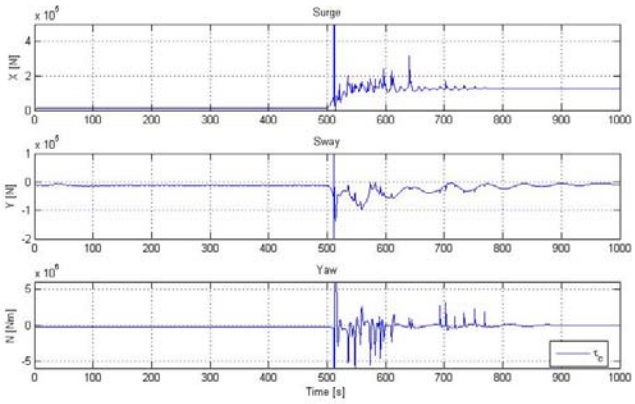

Figure 40 Control forces

Figure 40 shows the commanded control forces, were the switch to the WOPC controller is easily spotted by peaks in all three control directions (surge, sway and yaw). This could be avoided using bumpless transfer, but is not considered any further in this thesis. The control forces in yaw are acting very aggressively in the period after the switch. This is expected as the vessel would need to turn the bow up against the drifting ice. However, the control forces are very rapidly changing, and a better tuning of the controller gains would probably yield a more smooth command signal.

5.5 Discussion

The simulation using a regular open water controller (case 1) showed that the vessel was capable of keeping the position when the drifting ice hit head on, but with relatively large deviations from the desired position. The position errors were most significant in surge direction, as we would expect.

Case 2 shows that using the supervisory-switched control with an observer with ice load estimation and increased gains for the level ice controller as well as integrator reset when switching from level ice to open water controller, the position errors are reduced. The increased controller gains reduce the distance the vessel is pushed back by the ice at the initial ice edge contact and the integrator reset when the vessel leaves the ice eliminates the vessel overshoot. Instead, the vessel is again pushed back by the wind, current and ice friction loads. This position deviation is, however, smaller than the overshoot experienced without switching.

When the level ice sheet hits the vessel from an angle, the supervisory control using the level ice PID controller does not perform satisfactory. Even though the commanded heading is only 20 degrees off the ice drift direction the vessel is not able to keep the heading angle. Due to the extreme ice loads in sway and, most importantly, in yaw, the vessel lose control of the situation and is not able to keep the position.

It is noted that the drift angle does not seem to reduce the detection time. If the vessel was subject to a beam sea condition, one would maybe have to include roll motion in the detection algorithm as the waves would not cause much pitch motion.

The simulation using WOPC controller shows improved performance over the PID controller, and is actually performing better than the PID controller in simulation case 2 also with position deviations of less than one meter. This suggests that there is much to gain by researching alternative controller structures tailored for performance in ice conditions.

6 Conclusion and further work

This chapter concludes the report and gives a summary of the main findings of the thesis as well as proposals for further work.

6.1 Conclusion

A supervisory-switched control system for use in DP systems for arctic areas was developed and simulated on a supply vessel in MCSim.

A method for estimation of operating regime based on FFT analysis of measurements of vessel pitch motion was developed through a simulation study of the vessel in level ice. The ice model proposed by Røset (2009) was used for calculation of ice loads. Only open water and level ice conditions were considered due to limitations in broken ice load calculation algorithm. A variation of parameters showed that the detection time from open water to level ice condition was dependent on the pitch measurement buffer size where it was found that using a buffer length of 1024 samples, the supervisor was able to detect the difference between open water end level ice frequency spectra. Due to low resolution of the FFT, lower buffer lengths were not able to separate the two spectra with sufficient accuracy. A simulation study showed that reliable detection from open water to level ice was achieved in 12 seconds with appropriate tuning of buffer length and forgetting factors in the monitoring signal generator.

Observers tailored for ice conditions were presented. These were essentially open water nonlinear passive observers with increased bias estimation gains were the wave filtering was disregarded. PID controllers with increased gains in combination with the ice observers were used in a simulation study where a level ice sheet hit the vessel head on. The supervisory-switched control system reduced the position deviation in the ice drift direction from 4 meters to 1.5 meters.

A simulation of the vessel being hit by a level ice sheet from an angle showed that the PID controllers were not able to maintain the vessel position. When the level ice PID controller was substituted with a weather-optimal positioning controller (WOPC), the vessel was able to rotate the bow up against the drifting ice and showed good station keeping abilities. The WOPC controller was implemented without bumpless transfer, resulting in a sudden peak in control command at the switching instant. In addition, it was observed very aggressive control commands in yaw moment after the switch. A controller with a more relaxed tuning of the controller gains is believed to give a more smooth control command.

The bumpless transfer scheme was used in the switching between PID controller but was shown to provide very sudden transfer of authority from one controller to the other. A control model of the vessel which is better suited for use in the bumpless transfer scheme may provide a more smooth transition. Other selections of design matrices may also improve the controller behavior at the switching instants.

6.2 Recommendations for further work

The broken ice load MCSim module proposed by Stuberg (2009) should be extended to six degrees of freedom such that it would be possible to study vessel pitch motion and simulate the transition from

open water, through broken ice into level ice using the proposed detection method. The broken ice module should also be expanded to include wave motion of the broken ice floes as it is not feasible to simulate the ice floes in waves with the current modeling. To create an even more realistic simulation scenario, other ice regime modules should such as ice ridge models should be included in MCSim. Theory and for gradually reduction of wave motion s the vessel proceeds into an ice regime should be investigated and implemented in MCSim.

To validate the performance of the supervisory-switched controller, model tests of the vessel in ice using supervisory DP control should be performed.

The bumpless transfer scheme presented in this thesis has a few weak points, and should be further investigated to provide the desired functionality.

The controllers considered in this thesis was only open water PID controllers (except the WOPC controller) with more aggressive gain tuning. More specialized controllers taking the ice conditions into consideration should be developed. In light of the good results using the weather optimal positioning control scheme (WOPC), a further study of its applicability in ice should be performed.

7 References

Bjerkås, M., Skiple, A. & Røe, O.I., 2007. Applications of continuous wavelet transforms on ice load signals. *Engineering Structures*, 29(7), pp.1450-56.

Blanke, M., Kinnaert, M., Lunze, J. & Staroswiecki, M., 2006. *Diagnosis and Fault-Tolerant Control*. 2nd ed. Springer Berling Heidelberg.

Fossen, T.I., 2002. *Marine Control Systems: Guidance, Navigation and Control of Ships, Rigs and Underwater Vehicles*. 1st ed. Trondheim: Marine Cybernetics.

Fossen, T.I. & Strand, J.P., 2000. Nonlinear passive weather optimal positioning control (WOPC) system for ships and rigs: experimental results. *Automatica*, (37), pp.701-15.

Hespanha, J.P., 1998. *Logic-Based Switching Algorithms in Control*. PhD Thesis. New Haven, Connecticut: Yale University.

Hespanha, J.P., 2002. Tutorial on Supervisory Control. In *Lecture notes for the workshop Control using Logic and Switching for the 40th Conference on Decision and Control*. Orlando, Florida, 2002.

Hespanha, J.P., Liberzon, D. & Morse, A.S., 2003. Overcoming the limitations of adaptive control by means of logic-based switching. *Systems and Control Letters*, April. pp.49-65.

Keinonen, A.J., 2008. Ice Management for Ice Offshore Operations. In *Offshore Technology Conference*. Houston, 2008.

Khalil, H.K., 2002. *Nonlinear systems*. 3rd ed. Upper Saddle River, NJ: Prentice Hall.

Kuehnlein, W.L., 2009. Philosophies for Dynamic Positioning in Ice-Covered Waters. In *Offshore Technology Conference*. Houston, 2009.

Lewis, E.O., Currie, B.W. & Haykin, S., 1987. *Detection and classification of ice*. Research studies press.

Löfberg, J., 2004. YALMIP: A toolbox for modeling and optimization in MATLAB. In *CACSD Conference*. Taipei, Taiwan, 2004.

Nguyen, T.D., 2005. *Design of Hybrid Marine Control Systems for Dynamic Positioning*. PhD Thesis. Singapore: National University of Singapore.

Røset, E.S., 2009. *Dynamic Positioning of Marine Vessels in Level Ice*. Master Thesis. Trondheim: Norwegian University of Science and Technology.

Sandven, S. & Johannessen, O.M., 2006. Sea ice monitoring by remote sensing. In J.F.R. Gower, ed. *Manual of remote sensing: Remote sensing of the marine environment*. 3rd ed. The American society for photogrammetry & remote sensing. pp.241-83.

Skogvold, M., 2009. *Hybrid control for dynamic positioning systems in arctic areas*. Project thesis. Trondheim: NTNU.

Stuberg, P., 2009. *Dynamic Positioning in an Arctic Environment*. Master Thesis. Trondheim: Norwegian University of Science and Technology.

Sørbø, A.H., 2008. *Dynamic Positioning in an Arctic Environment*. Master Thesis. Trondheim: Norwegian University of Science and Technology.

Sørensen, A.J., 2005. *Marine Cybernetics: Modelling and control*. Lecture notes. Trondheim: Norwegian university of science and technology.

United States Geological Survey, 2008. *90 Billion Barrels of Oil and 1670 Trillion Cubic Feet of Natural Gas Assessed in the Arctic*. [Online] Available at: http://www.usgs.gov/newsroom/article.asp?ID=1980 [Accessed 13 June 2010].

Zaccarian, L. & Teel, A., 2001. Anti-Windup, Bumpless Transfer andreliable designs: a model based approach. In *American Control Conference*. Arlington, VA, 2001.

Zaccarian, L. & Teel, A.R., 2002. A common framework for anti-windup, bumpless transfer and reliable designs. *Automatica*, 38(10), pp.1735-44.

Åstrøm, K.J. & Wittenmark, B., 1995. *Adaptive Control*. 2nd ed. Addison-Wesley Publishing Company, Inc.

Appendix A Weather optimal positioning control

A.1 WOPC controller equations

By defining new state vectors

$$\mathbf{x} \triangleq [\rho \quad \gamma \quad \psi]^T \tag{A.1}$$

$$\mathbf{p}_0 \triangleq [x_0 \quad y_0]^T, \tag{A.2}$$

and introducing new variables for tracking of a desired reference trajectory $\mathbf{x}_d = [\rho_d \quad \gamma_d \quad \psi_d]^T$,

$$\mathbf{z}_1 \triangleq \mathbf{x} - \mathbf{x}_d \tag{A.3}$$

$$\mathbf{z}_2 \triangleq \dot{\mathbf{x}} - \dot{\mathbf{x}}_r = \dot{\mathbf{z}}_1 + \Lambda \mathbf{z}_1, \tag{A.4}$$

and the virtual reference trajectory

$$\dot{\mathbf{x}}_r \triangleq \dot{\mathbf{x}}_d - \Lambda \mathbf{z}_1. \tag{A.5}$$

A ship control plant model is transformed into polar coordinates:

$$\mathbf{M}_x \ddot{x} + \mathbf{C}_x \dot{x} + \mathbf{D}_x \dot{x} = \mathbf{T}^{-T} \tau + \mathbf{T}^{-T} q(\nu, x, \dot{p}_0, \ddot{p}_0) + \mathbf{T}^{-T} w. \tag{A.6}$$

Then, the following equations gives the weather optimal positioning controller:

$$\dot{\hat{F}}_e = \sigma \phi^T \mathbf{T}^{-1} \mathbf{z}_2 \tag{A.7}$$

$$\dot{\tilde{\mathbf{p}}} = -k_0 \tilde{\mathbf{p}} + \mathbf{L}^T \mathbf{R}(\gamma) \mathbf{H}(\rho) \mathbf{z}_2 \tag{A.8}$$

$$\tau = \mathbf{T}^T (\mathbf{M}_x \ddot{\mathbf{x}}_r + \mathbf{C}_x \dot{\mathbf{x}}_r + \mathbf{D}_x \dot{\mathbf{x}}_r - \mathbf{K}_p \mathbf{z}_1 - \mathbf{K}_d \mathbf{z}_2) - \mathbf{q}(\bullet) - \phi \hat{F}_e - \mathbf{T}^T \mathbf{H}^T(\rho) \mathbf{R}^T(\gamma) \mathbf{L} \tilde{\mathbf{p}}, \tag{A.9}$$

where

$$\mathbf{M}_x = \mathbf{T}^{-T}(x) \mathbf{M} \mathbf{T}^{-1}(x) \tag{A.10}$$

$$\mathbf{C}_x = \mathbf{T}^{-T}(x) (\mathbf{C}(\nu) - \mathbf{M} \mathbf{T}^{-1}(x) \dot{\mathbf{T}}(x)) \mathbf{T}^{-1}(x) \tag{A.11}$$

$$\mathbf{D}_x = \mathbf{T}^{-T}(x) \mathbf{D}(\nu) \mathbf{T}^{-1}(x) \tag{A.12}$$

$$\mathbf{q}(\bullet) = \mathbf{M} \mathbf{R}^T(\psi) \mathbf{L} \ddot{\mathbf{p}}_0 + \mathbf{M} \dot{\mathbf{R}}^T(\psi) \mathbf{L} \dot{\mathbf{p}}_0 + [\mathbf{C}(\nu) + \mathbf{D}(\nu)] \mathbf{R}^T(\psi) \mathbf{L} \dot{\mathbf{p}}_0 \tag{A.13}$$

$$\ddot{p}_0 = \ddot{p}_d - k_0(\dot{p} - \dot{p}_d) - \mathbf{L}^T\mathbf{R}(\gamma)\mathbf{H}(\rho)\ddot{x}_r - \mathbf{L}^T\dot{\mathbf{R}}(\gamma)\mathbf{H}(\rho)\dot{x}_r - \mathbf{L}^T\mathbf{R}(\gamma)\dot{\mathbf{H}}(\rho)\dot{x}_r \tag{A.14}$$

$$p = \mathbf{L}^T\eta \tag{A.15}$$

$$\mathbf{T} = \mathbf{H}^{-1}(\rho)\mathbf{R}^T(\gamma)\mathbf{R}(\psi) = \mathbf{H}^{-1}(\rho)\mathbf{R}^T(\gamma - \psi) \tag{A.16}$$

$$\dot{\mathbf{T}} = -\dot{\rho}\Pi(\rho) - (\dot{\gamma} - \dot{\psi})\mathbf{H}^{-1}(\rho)\mathbf{S}\mathbf{R}(\gamma - \psi) \tag{A.17}$$

$$\dot{\mathbf{R}}(\alpha) = \dot{\alpha}\mathbf{R}(\alpha)\mathbf{S} \tag{A.18}$$

$$\mathbf{R}(\alpha) = \begin{bmatrix} \cos(\alpha) & -\sin(\alpha) & 0 \\ \sin(\alpha) & \cos(\alpha) & 0 \\ 0 & 0 & 1 \end{bmatrix} \tag{A.19}$$

$$\mathbf{H} = \begin{bmatrix} 1 & 0 & 0 \\ 0 & \rho & 0 \\ 0 & 0 & 1 \end{bmatrix} \tag{A.20}$$

$$\mathbf{S} = \begin{bmatrix} 0 & 1 & 0 \\ -1 & 0 & 0 \\ 0 & 0 & 0 \end{bmatrix} \tag{A.21}$$

$$\mathbf{E} = \begin{bmatrix} 1 & 0 & 0 \\ 0 & 0 & 1 \end{bmatrix} \tag{A.22}$$

$$\mathbf{L} = \begin{bmatrix} 1 & 0 \\ 0 & 1 \\ 0 & 0 \end{bmatrix} \tag{A.23}$$

$$\phi = \begin{bmatrix} -1 & 0 & 0 \end{bmatrix}^T. \tag{A.24}$$

And the controller design gain matrices

$$\mathbf{K}_p = \begin{bmatrix} k_{p1} & 0 & 0 \\ 0 & 0 & 0 \\ 0 & 0 & k_{p3} \end{bmatrix} \tag{A.25}$$

$$\mathbf{K}_d = \begin{bmatrix} k_{d1} & 0 & 0 \\ 0 & k_{d2} & 0 \\ 0 & 0 & k_{d3} \end{bmatrix} \tag{A.26}$$

$$\Lambda = \begin{bmatrix} \lambda_1 & 0 & 0 \\ 0 & 0 & 0 \\ 0 & 0 & \lambda_3 \end{bmatrix}. \tag{A.27}$$

Appendix B Control system parameters

B.1 Open water

B.1.1 Observer

Observer gain matrices used for open water case:

$$\mathbf{K}_1 = \begin{bmatrix} diag\begin{bmatrix} -54 & -54 & 54 \end{bmatrix} \\ diag\begin{bmatrix} 1.68 & 1.68 & 1.68 \end{bmatrix} \end{bmatrix} \tag{B.1}$$

$$\mathbf{K}_2 = diag\begin{bmatrix} 28.02 & 28.02 & 28.02 \end{bmatrix} \tag{B.2}$$

$$\mathbf{K}_3 = diag\begin{bmatrix} 4e6 & 4e6 & 4e8 \end{bmatrix} \tag{B.3}$$

$$\mathbf{K}_4 = diag\begin{bmatrix} 4e7 & 4e7 & 4e9 \end{bmatrix} \tag{B.4}$$

$$T = diag\begin{bmatrix} 1000 & 1000 & 1000 \end{bmatrix} \tag{B.5}$$

B.1.2 Controller

$$\mathbf{K}_p = \begin{bmatrix} 2.86e4 & 0 & 0 \\ 0 & 4.66e4 & 1.14e6 \\ 0 & -2.56e4 & 3.72e6 \end{bmatrix} \tag{B.6}$$

$$\mathbf{K}_i = \begin{bmatrix} 2.00e2 & 0 & 0 \\ 0 & 6.70e2 & 2.46e3 \\ 0 & -2.25e2 & 7.34e3 \end{bmatrix} \tag{B.7}$$

$$\mathbf{K}_d = \begin{bmatrix} 5.44e5 & 0 & 0 \\ 0 & 1.07e6 & 1.74e7 \\ 0 & -4.07e5 & 1.14e8 \end{bmatrix} \tag{B.8}$$

B.2 Level ice

B.2.1 Observer

Observer gain matrices used for level ice case:

$$\mathbf{K}_2 = diag\begin{bmatrix} 28.02 & 28.02 & 28.02 \end{bmatrix} \tag{B.9}$$

$$\mathbf{K}_3 = diag\begin{bmatrix} 4e6 & 4e6 & 4e8 \end{bmatrix} \tag{B.10}$$

$$\mathbf{K}_{51} = diag\begin{bmatrix} 3e6 & 6e5 & 1e9 \end{bmatrix} \tag{B.11}$$

$$T_{ice} = diag\begin{bmatrix} 500 & 500 & 500 \end{bmatrix} \tag{B.12}$$

B.2.2 PID Controller

$$\mathbf{K}_p = \begin{bmatrix} 5.71e4 & 0 & 0 \\ 0 & 9.31e4 & 2.28e6 \\ 0 & -5.11e4 & 7.44e6 \end{bmatrix} \tag{B.13}$$

$$\mathbf{K}_i = \begin{bmatrix} 8.00e2 & 0 & 0 \\ 0 & 2.68e3 & 9.85e3 \\ 0 & -8.99e2 & 2.94e4 \end{bmatrix} \tag{B.14}$$

$$\mathbf{K}_d = \begin{bmatrix} 5.44e5 & 0 & 0 \\ 0 & 1.07e6 & 1.73e7 \\ 0 & -4.07e5 & 1.14e8 \end{bmatrix} \tag{B.15}$$

B.2.3 WOPC controller

$$\mathbf{K}_p = diag\begin{bmatrix} 1e7 & 0 & 1e8 \end{bmatrix} \tag{B.16}$$

$$\mathbf{K}_d = diag\begin{bmatrix} 5e6 & 1e9 & 1e9 \end{bmatrix} \tag{B.17}$$

$$\Lambda = diag\begin{bmatrix} 1 & 0 & 1 \end{bmatrix} \tag{B.18}$$

$$k_0 = 0.1 \tag{B.19}$$

$$\sigma = 1e4 \tag{B.20}$$

$$p_{0,init} = \begin{bmatrix} 12.5 & 25 \end{bmatrix}^T \tag{B.21}$$

$$\rho_d = \sqrt{25^2 + 12.5^2} \tag{B.22}$$

B.3 Supervisor

Supervisor parameters used in the simulations:

Forgetting factors: $$\lambda = \begin{bmatrix} 0.10 & 0.10 \end{bmatrix} \tag{B.23}$$

Hysteresis constant: $$h = 0.1 \tag{B.24}$$

Initial monitoring signal values: $$\mu_{init} = \begin{bmatrix} 0 & 10 \end{bmatrix} \tag{B.25}$$

Bufferlength: $$N_{FFT} = 1024 \tag{B.26}$$

Buffer overlap: $$1022 \tag{B.27}$$

Sample period: $$T_s = 0.01[s] \tag{B.28}$$

Appendix C Contents of the attached CD

C.1 MCSim Simulink model

The MCSim Simulink model used in the simulation study with all necessary configuration files is included in the folder *MCSim*

C.2 Results

Selected results from the simulation study are included in *.mat files in the folder *Results*

NTNU

Norwegian University of
Science and Technology